



<https://technobius.kz/>

e-ISSN
2789-7338

Technobius

A peer-reviewed open-access journal

Technobius, LLP

Volume 2, No. 2, 2022



Technobius

Volume 2, No. 2, 2022



A peer-reviewed open-access journal registered by the Ministry of Information and Social Development of the Republic of Kazakhstan, Certificate № KZ00VPY00039799 dated 7.09.2021

ISSN (Online): 2789-7338

Thematic Directions: Construction and Materials Science




Publisher: Technobius, LLP

Address: 17A Momysuly street, office 22, 010000, Nur-Sultan, Republic of Kazakhstan




Editor-in-Chief:




   *Yelbek Utepov*, PhD, Professor, Department of Civil Engineering, L.N. Gumilyov Eurasian National University, Astana, Kazakhstan




Technical Editor:




   *Assel Tulebekova*, PhD, Associate Professor, Department of Civil Engineering, L.N. Gumilyov Eurasian National University, Astana, Kazakhstan




Editors:



   *Yuri Pukhareenko*, Doctor of Technical Sciences, Professor, Department of Building Materials Technology and Metrology, Saint Petersburg State University of Architecture and Civil Engineering, Saint Petersburg, Russian Federation




   *Askar Zhussupbekov*, Doctor of Technical Sciences, Professor, Department of Civil Engineering, L.N. Gumilyov Eurasian National University, Astana, Kazakhstan




   *Evgeniya Tkach*, Doctor of Technical Sciences, Professor, Department of Building Materials Science, Moscow State University of Civil Engineering, Moscow, Russian Federation




   *Ignacio Menéndez Pidal de Navascués*, Doctor of Technical Sciences, Professor, Department of Civil Engineering, Technical University of Madrid, Madrid, Spain

   *Irina Aubakirova*, Candidate of Technical Sciences, Associate Professor, Department of Building Materials Technology and Metrology, Saint Petersburg State University of Architecture and Civil Engineering, Saint Petersburg, Russian Federation

   *Zeljko Kos*, PhD, Assistant Professor, Department of Civil Engineering, University North, Varaždin, Croatia

   *Aleksej Aniskin*, Candidate of Technical Sciences, Assistant Professor, Department of Civil Engineering, University North, Varaždin, Croatia

   *Daniyar Akhmetov*, Doctor of Technical Sciences, Associate Professor, Department of Construction and Building materials, Satbayev University, Almaty, Kazakhstan

   *Zhanbolat Shakhmov*, PhD, Associate Professor, Department of Civil Engineering, L.N. Gumilyov Eurasian National University, Astana, Kazakhstan

Copyright: © Technobius, LLP

Contacts: Website: <https://technobius.kz/>
E-mail: technobius.research@gmail.com

CONTENTS

Title and Authors	Category	No.
Modeling the impact of soil cohesiveness on embankment stability under rapid drawdown <i>Timoth Mkilima</i>	<i>Construction</i>	0016
Numerical modeling of the interaction of bored micro piles with the substrate <i>Abdulla Omarov, Gulshat Tleulnova</i>	<i>Construction</i>	0017
Defects in a dilapidated building resulting in loss of bearing capacity of supporting structures <i>Alizhan Kazkeyev, Daniyar Kenzhebekov, Nursultan Tattikulov</i>	<i>Construction</i>	0018
On-site pilot testing of maturity sensors in conjunction with ambient condition monitoring device to get an insight into the concrete strength gain process <i>Yelbek Utepov, Shyngys Zharassov</i>	<i>Construction, Materials Science</i>	0019
Use of recycled waste in the production of building materials <i>Kapar Aryngazin, Assem Abisheva</i>	<i>Materials Science</i>	0020



Modeling the impact of soil cohesiveness on embankment stability under rapid drawdown

 Timothy Mkilima*

Ardhi University, Plot Number 3 Block L, Observation Hill, P. O. Box 35176, Dar Es Salaam, Tanzania.

Abstract. For embankment slope stability, soil cohesivity is one of the most important shear strength parameters. The effect of cohesiveness on the slope stability of a homogeneous embankment dam under rapid drawdown loading conditions was examined in this study. With the use of numerical modeling in GeoStudio, different situations were explored based on cohesiveness (0 kN/m², 5 kN/m², 10 kN/m² and 15 kN/m²) under a 1 m per day drawdown rate. The factor of safety value obtained from the long-term steady-state condition under 15 kN/m² cohesion was equivalent to a 116.8% increase from the one obtained under 0 kN/m² cohesion. The factor of safety values obtained after subjecting the embankment to different soil cohesion levels yielded a p-value of 1.91×10^{-41} , according to the Analysis of Variance. The calculated p-value (alpha value) is less than 0.05, suggesting that the differences between the examined cohesiveness values based on the list of the factor of safety values are statistically significant. The findings derived in this study show that it is significant to capture the effect of material characteristics during the design phase of an embankment dam.

Keywords: embankment, numerical modeling, factor of safety, soil cohesiveness, slope stability.

1. Introduction

Soil cohesiveness is defined as the ability of soil particles to be structured or arranged in a united manner, with close or strong internal connections. Cohesion is the component of a rock's or soil's shear strength that is unaffected by interparticle friction [1]. In general, shear strength under zero normal stress, or the intersection of a material's failure envelope with the shear stress axis in the shear stress-normal stress space, is referred to as cohesion in soil mechanics [2]. On the other hand, drained cohesion is defined as cohesiveness under saturated drained conditions, while apparent cohesion is defined as cohesion under variably saturated conditions [3].

The potential relationship governing the compressive stress (p) as well as the corresponding shear strength (s) in cohesive soils is commonly considered to be described by an empirical equation known as Coulomb's equation as highlighted in Equation 1 [1].

$$s = c + p \tan \varphi \quad (1)$$

Whereby: c is the shear cohesion, φ is the angle of internal friction.

The technique of estimating and assessing how much stress a given slope can handle before failing is known as slope stability [4]. Commercial highways, dams, excavated slopes, and soft rock walks in reservoirs, forests, and parks are examples of common slopes. Slope stability analysis is important for civil and geotechnical engineers planning construction for highways, dams, embankments, and other excavated slopes, because failing to comprehend slope stability can lead to landslides, unwanted movement, and injury to both property and people [5].

Furthermore, in the case of embankment slope stability, a single failure surface can be examined using several approaches that have evolved through time to determine its Factor of Safety (FS) [6]. An engineer must choose the most critical surface, i.e. the one with the lowest FS when analyzing the stability of either man-made or natural slopes [7]. Designers must consider whether the

slope should be reinforced to meet the minimum needed FS after selecting this surface [8]. Slope stability concerns have caused projects to be drastically altered in the past, with the decision-making process being both a technical and a financial issue [9].

Prior to the development of computational tools, determining the critical failure surface was a difficult task that necessitated several, time-consuming manual analyses. Nonetheless, technological improvements have made it possible to carry out a variety of examinations [10]. As a result, after numerous rounds, the critical failure surface and its FS can be easily determined. The Mohr-Coulomb criterion is commonly used to incorporate the material(s)' cohesion and friction.

Clay, silty clay, sandy clay, clay loam, and, in rare circumstances, silty clay loam and sandy clay loam are examples of cohesive soils. Noncohesive soils include clean sand and gravel. If the silt is nonplastic, sand and gravel containing silt may be noncohesive, necessitating the measurement of the Atterberg limits. Cohesive behavior would be observed in sand and gravel with clay or plastic silt. In geotechnical engineering, numerical modeling is commonly used to study the responses of infrastructures in civil engineering [11]. To cope with various geotechnical difficulties, a variety of handmade or commercialized numerical codes are available.

The impact of soil cohesiveness on embankment stability under coupled fast drawdown analysis is examined in the present study. In GeoStudio software, the topic is investigated using the finite element method.

2. Materials and Methods

2.1 General description of the numerical simulation

Under the steady-state condition and rapid drawdown rate, finite element method analyses were used to explore the effect of cohesion on slope stability (1 m per day). Different cases were considered, as determined by soil cohesion (0 kN/m², 5 kN/m², 10 kN/m², and 15 kN/m²). The GeoStudio software suite was used to perform the numerical modeling (GeoStudio 2018 R2 v9.1.1.16749). The GeoStudio's SEEP/W and SLOPE/W sub-units were primarily employed for seepage and slope stability analyses, respectively.

2.2 Embankment geometry

In all of the cases studied, the embankment geometry was kept constant while the material cohesiveness was changed to investigate its influence on the embankment stability. As illustrated in Figure 1, the embankment is roughly 68 meters wide at the base and 8 meters wide at the top, with a height of 11 meters. The reservoir's highest water level is 9 meters.

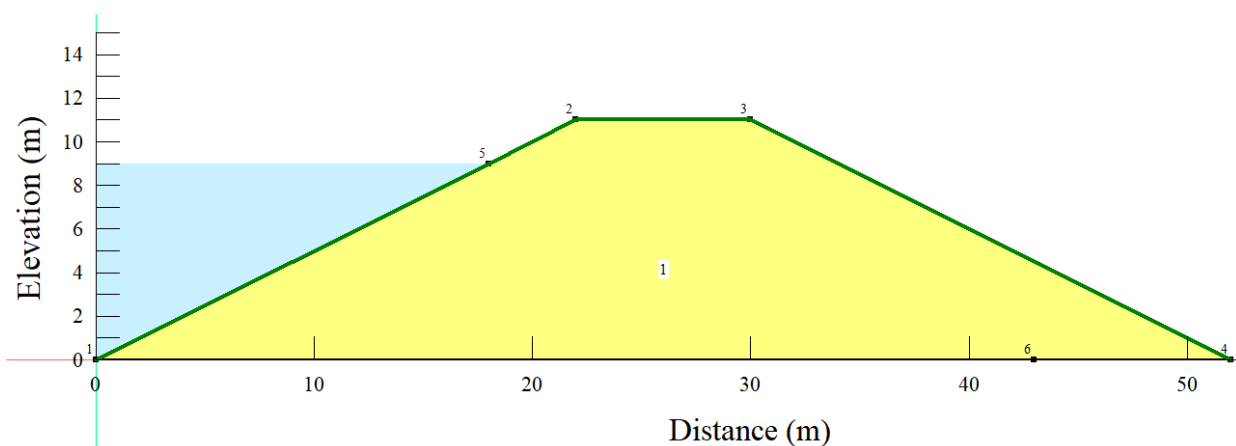


Figure 1 – Geometry of the study embankment

2.3 Soil material characteristics

To avoid any fluctuation and capture the influence of variations in the soil cohesion, the soil material parameters for the embankment were kept constant for all of the models analyzed. The soil

material parameters utilized in the seepage and slope stability analyses are summarized in Table 1. The major soil parameters in the model were saturated water content, coefficient of compressibility, conductivity, residual water content, soil unit weight, cohesion, and internal friction angle.

Table 1 – Soil material properties

Soil material properties	Symbol	Unit	Value
Saturated water content	θ_s	%	43
Coefficient of volume compressibility	M_v	m ² /kN	2×10^{-4}
Saturated conductivity	K_{sat}	m/s	1×10^{-6}
Residual water content	θ_r	%	5.5
Soil unit weight	γ	kN/m ³	20
Cohesion	c'	kN/m ²	0, 5, 10, 15
Internal friction angle	ϕ'	degrees	27

2.4 Statistical analysis

To test if the differences between sets of data were statistically significant, a single-factor Analysis of Variance (ANOVA) was utilized. This method examines the amounts of variance within each group using samples from each group. The significance level was calculated using the combination of alpha (0.05) and p-value to be more specific.

3. Results and Discussion

The model embankment was initially put through a series of long-term steady-state investigations with varying cohesion levels. Figure 2 shows that as the soil cohesiveness increased, the long-term steady-state factor of safety values increased as well. The factor of safety value obtained from the 5 kN/m² cohesiveness was equivalent to a 52.6 % increase over that obtained from the 0 kN/m² cohesion.

Meanwhile, the 10 kN/m² cohesiveness factor of safety value was equivalent to a 22.2 % increase over the 5 kN/m² cohesion. In addition, the factor of safety value obtained from the 15 kN/m² cohesiveness was roughly 16.2 % higher than that obtained from the 10 kN/m² cohesion. The results also show that as the soil cohesiveness in the embankment increases, the disparity in terms of factor of safety values between cohesion values under long-term steady-state conditions decreases.

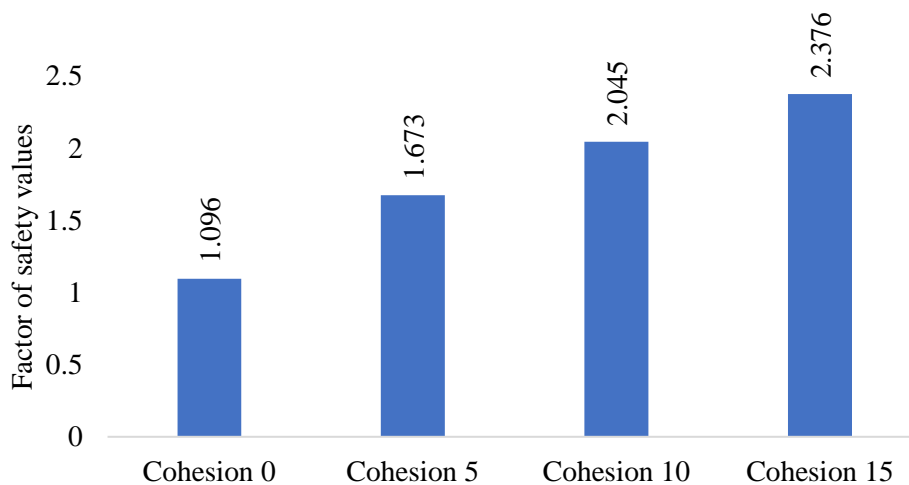


Figure 2 – Factor of safety values from long-term steady-state conditions

When the embankment was subjected to 0 kN/m² cohesion and a 1 m per day drawdown rate, Figure 3 shows the trend of the factor of safety values. The minimum factor of safety (attained on the eighth day of drawdown) was roughly 0.749, as shown in Figure 3. The factor of safety value obtained

is 31.66 % lower than that obtained using the long-term steady-state condition and 0 kN/m² cohesion. Furthermore, the minimum factor of safety value is less than one, indicating that the embankment has failed.

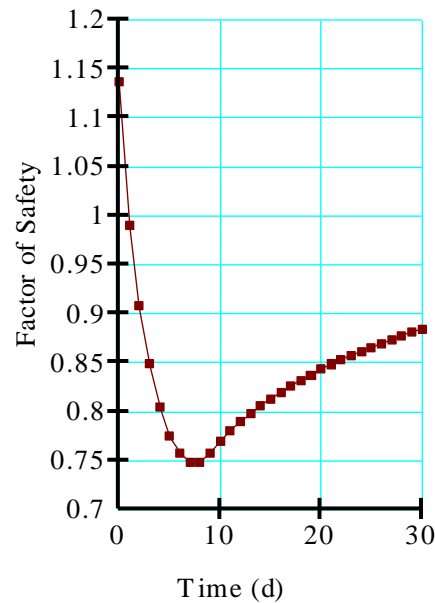


Figure 3 – Graph of the factor of safety values from 0 kN/m² cohesion material

Figure 4 depicts the factor of safety values obtained from a 1 m per day drawdown rate and a 5 kN/m² cohesiveness. In contrast to the minimal factor of safety value obtained from the 0 kN/m² cohesion, Figure 4 shows that the 5 kN/m² cohesion generated a minimum factor of safety greater than 1 (1.058), which can be regarded as safer. The factor of safety is 36.76 % lower than calculated using the long-term steady-state condition and 5 kN/m² cohesion.

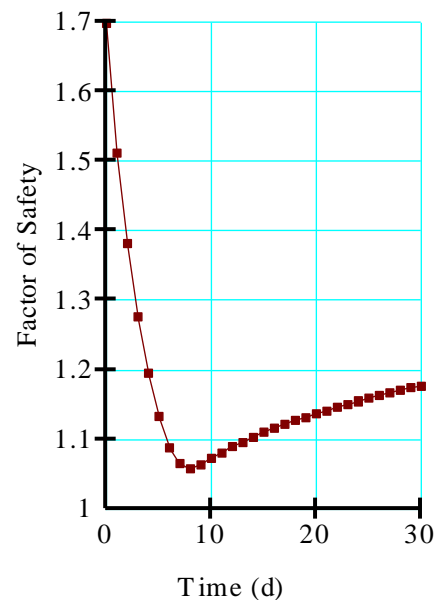


Figure 4 – Graph of the factor of safety values from 5 kN/m² cohesion material

The factor of safety values from the 1 m per drawdown rate and 10 kN/m² soil cohesiveness are summarized in Figure 5. It was discovered that a minimal factor of safety value of about 1.293 was obtained. The factor of safety value obtained is 36.77 % lower than that obtained using the long-term steady-state condition and 10 kN/m² cohesion.

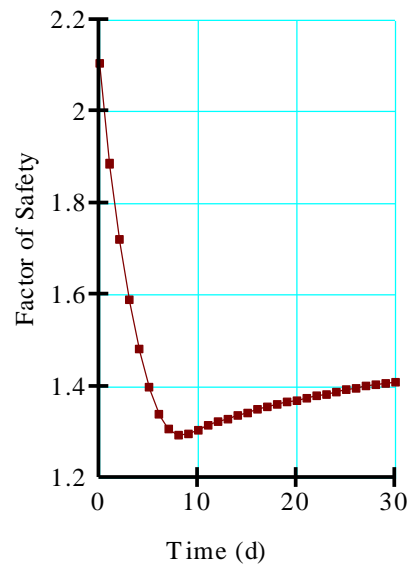


Figure 5 – Graph of the factor of safety values from 10 kN/m² cohesion material

In addition, Figure 6 summarizes the factor of safety values derived from the 1 m per day drawdown rate and 15 kN/m² soil cohesion. A minimal factor of safety of 1.516 was attained using a combination of 10kN/m² cohesiveness and a quick drawdown rate. The factor of safety value obtained is 36.20 % lower than that obtained using the long-term steady-state condition and 15 kN/m² cohesion. In general, the results reveal further that under a constant drawdown rate, the increase in soil cohesion increases the minimum factor of safety values. The results in this study comprehend with the study conducted by [12]; whereby, it was observed that changes in cohesion had a significant effect on the factor of safety.

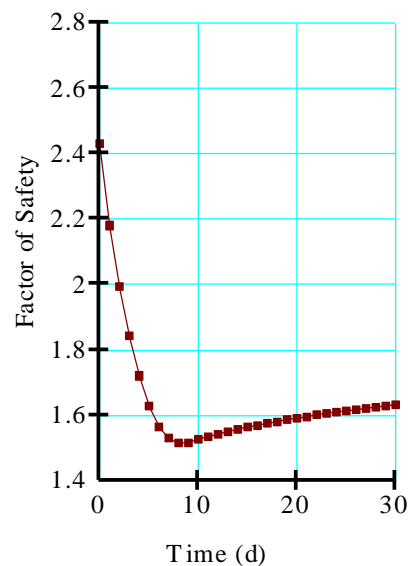


Figure 6 – Graph of the factor of safety values from 15 kN/m² cohesion material

ANOVA was used to see if there were any significant changes in the retrieved factor of safety values from the examined operating levels and drawdown rates. From day 0 (defined by the long-term steady-state condition) until day 30 of the rapid drawdown, a total of 31 factor of safety values were considered.

On the examined cohesion values under 1 m per day drawdown rate, a single-factor ANOVA with an alpha value of 0.05 was performed; the results of the ANOVA are reported in Table 2. The factor of safety values based on the investigated cohesion values generated a p-value of 1.91×10^{-41} , as shown in Table 2. The obtained p-value (alpha value) is less than 0.05, indicating that the variations

in the list of the factor of safety values from the investigated cohesion values are statistically significant. This was a crucial part of the study since it allowed us to see if the differences in factor of safety values across the cohesion values investigated were substantial [13].

Table 2 – Results from Analysis of Variance

ANOVA: Single Factor						
SUMMARY						
Groups	Count	Sum	Average	Variance		
Cohesion (0 kN/m ²)	31	26.07	0.84	0.0058		
Cohesion (5 kN/m ²)	31	36.27	1.17	0.0182		
Cohesion (10 kN/m ²)	31	44.11	1.42	0.0315		
Cohesion (15 kN/m ²)	31	51.27	1.65	0.0403		
ANOVA						
Source of Variation	SS	df	MS	F	P-value	F crit
Between Groups	11.32	3	3.77	157.53	1.91 x 10 ⁻⁴¹	2.68
Within Groups	2.87	120	0.024			
Total	14.19	123				

Figure 7 summarizes the minimum factor of safety values from the investigated cohesion values. From Figure 7, it can be seen that the minimum factor of safety values were decreasing with the decrease in the soil cohesion. It is also important to note that, the minimum factor of safety values were retrieved from the 1 m per day drawdown rate.

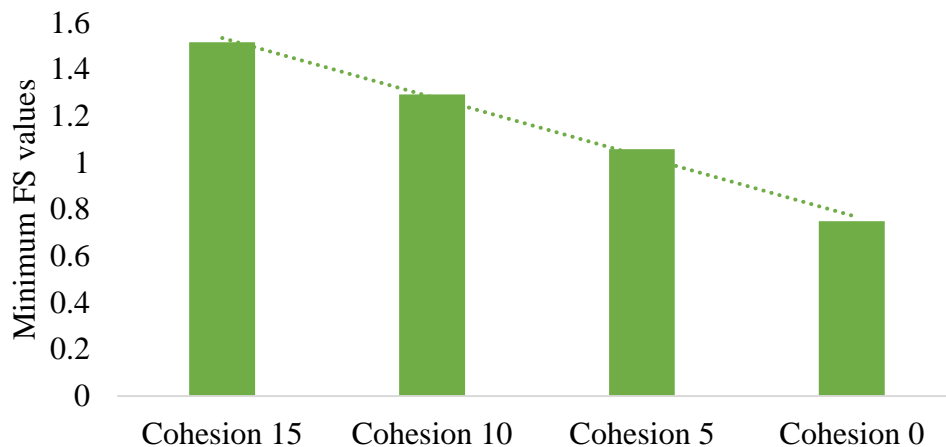


Figure 7. Summary of the minimum factor of safety values from the studied cohesion values

4. Conclusions

Under rapid drawdown loading conditions, the influence of cohesiveness on the slope stability of a homogeneous embankment dam was examined. The following may be concluded:

- According to the Analysis of Variance, the factor of safety values obtained after subjecting the embankment to varied soil cohesion levels provided a p-value of 1.91×10^{-41} .
- The estimated p-value (alpha value) is less than 0.05, indicating statistical significance between the analyzed cohesiveness values and the list of the factor of safety values.
- The factor of safety value obtained from the 5 kN/m² cohesiveness was 52.6 % higher than that obtained from the 0 kN/m² cohesiveness.
- Meanwhile, the factor of safety value of the 10 kN/m² cohesiveness was equivalent to a 22.2 % increase over the 5 kN/m² cohesion.
- Furthermore, the factor of safety value obtained from 15 kN/m² cohesiveness was approximately 16.2 % greater than that obtained from 10 kN/m² cohesiveness.

- The findings also reveal that as the embankment's soil cohesiveness increases, the discrepancy between cohesion values under long-term steady-state conditions reduces in terms of factor of safety values.
- Based on the results, it is significantly important to investigate the levels of soil cohesiveness during the design phase of an embankment dam.

References

1. Relationship between soil cohesion and shear strength / H. Yokoi // Soil Science and Plant Nutrition. — 1968. — Vol. 14, No. 3. — P. 89–93. <https://doi.org/10.1080/00380768.1968.10432750>
2. Mechanical behavior and durability of a typical frictional cohesive soil from Rio Grande do Sul/Brazil improved with Portland cement / T.F. de Souza Junior, K. Salvagni Heineck, C. Falavigna Silva, F. Dalla Rosa // Transportation Geotechnics. — 2022. — Vol. 34. — P. 100751. <https://doi.org/10.1016/j.trgeo.2022.100751>
3. The drained residual strength of cohesive soils / J.F. Lupini, A.E. Skinner, P.R. Vaughan // Géotechnique. — 1981. — Vol. 31, No. 2. — P. 181–213. <https://doi.org/10.1680/geot.1981.31.2.181>
4. A new approach for the slope stability analysis / H. Yang, J. Wang, Y. Liu // Mechanics Research Communications. — 2001. — Vol. 28, No. 6. — P. 653–669. [https://doi.org/10.1016/S0093-6413\(02\)00217-3](https://doi.org/10.1016/S0093-6413(02)00217-3)
5. Research on slope stability analysis of super-high dumping site based on cellular automaton / G. Wang, X. Kong, Y. Gu, C. Yang // Procedia Engineering. — 2011. — Vol. 12. — P. 248–253. <https://doi.org/10.1016/j.proeng.2011.05.039>
6. A novel reliability-based method of calibrating safety factor: Application to the cemented sand and gravel dams / N. Hao, X. Li, Y. Li, J. Jia, L. Gao // Engineering Geology. — 2022. — P. 106719. <https://doi.org/10.1016/j.enggeo.2022.106719>
7. Determination of critical slip surface and safety factor of slope using the vector sum numerical manifold method and MAX-MIN ant colony optimization algorithm / Y. Yang, W. Wu, J. Zhang, H. Zheng, D. Xu // Engineering Analysis with Boundary Elements. — 2021. — Vol. 127. — C. 64–74. <https://doi.org/10.1016/j.enganabound.2021.03.012>
8. Dynamics of Embankment Slope Stability under Combination of Operating Water Levels and Drawdown Conditions / Y.B. Utepov, A.K. Aldungarova, T. Mkilima, I.M. Pidal, A.S. Tulebekova, S.Z. Zharassov, A.K. Abisheva // Infrastructures. — 2022. — Vol. 7, No. 5. — P. 65. <https://doi.org/10.3390/infrastructures7050065>
9. The influence of material characteristics on dam stability under rapid drawdown conditions / Y. Utepov, Z. Lechowicz, A. Zhussupbekov, Z. Skutnik, A. Aldungarova, T. Mkilima // Archives of Civil Engineering Archives of Civil Engineering. — 2022. — Vol. LXVIII, No. 1. — P. 539–553. <https://doi.org/10.24425/ACE.2022.140184>
10. Toe drain size and slope stability of homogeneous embankment dam under rapid drawdown / T. Mkilima // Technobius. — 2021. — Vol. 1, № 3. — C. 0001. <https://doi.org/10.54355/tbus/1.3.2021.0001>
11. The potential effects caused by long-term water level changes on embankment slope stability under rapid drawdown / A.K. Aldungarova, Y. Utepov, T. Mkilima, A.S. Tulebekova, Sh.Zh. Zharassov // Bulletin of Kazakh Leading Academy of Architecture and Construction. — 2022. — Vol. 83, № 1. — C. 107–119. <https://doi.org/10.51488/1680-080X/2022.1-01>
12. Impact of shear strength parameters on slope stability / S. Harabinová, E. Panulinová // MATEC Web of Conferences. — 2020. — Vol. 310. — C. 00040. <https://doi.org/10.1051/mateconf/202031000040>
13. Real-time water quality monitoring through Internet of Things and ANOVA-based analysis: a case study on river Krishna / P.M. Pujar, H.H. Kenchannavar, R.M. Kulkarni, U.P. Kulkarni // Applied Water Science. — 2020. — Vol. 10, № 1. — C. 22. <https://doi.org/10.1007/s13201-019-1111-9>

Information about the author:

Timoth Mkilima – Research Fellow, Ardhi University, Plot Number 3 Block L, Observation Hill, P. O. Box 35176, Dar Es Salaam, Tanzania, tmkilima@gmail.com

Author Contributions:

Timoth Mkilima – concept, methodology, resources, data collection, testing, modeling, analysis, visualization, interpretation, drafting, editing, funding acquisition.

Received: 03.06.2022

Revised: 19.06.2022

Accepted: 21.06.2022

Published: 21.06.2022



Numerical modeling of the interaction of bored micro piles with the substrate

 Abdulla Omarov*,  Gulshat Tleulenova

Department of Civil Engineering, L.N. Gumilyov Eurasian National University, Nur-Sultan, Kazakhstan

*Correspondence: omarov_01@bk.ru

Abstract. The paper describes the results of a numerical simulation of micro-pile tests using the PLAXIS 2D software package. The purpose of the simulation in this article is to determine the bearing capacity of the micro pile in static tests. Axisymmetric models of a 500 mm wide and 31 m long micro pile were used in the calculation. The staged loading of the pile in the program was simulated by increasing the load on the pile by 145 kN. The main monitored calculation parameters were the magnitude of the applied load and the pile settlement. As a result, load-settlement diagrams were plotted from the pile tests. The bearing capacity of the piles was determined based on a numerical simulation of the pile and the ground in the PLAXIS 2D software package and compared with field data. This geotechnical investigation is important for understanding the soil-structure interaction on difficult and problematical soil ground conditions related to the construction sites.

Keywords: BDSLT, FEM, pile, load, PLAXIS 2D, soil.

1. Introduction

At present, numerical calculation methods, including finite element methods (FEM), finite difference methods (FD) and boundary element method (BEM) are applied for quantitative estimation of the deflectivity of heterogeneous soil masses interacting with underground structures of buildings and constructions. These methods are based on the joint solution of a system of differential equations of equilibrium, continuity and physical equations. The latter define the dependencies of the ground deformation on the stress state. Currently, there are different methods for describing the physical equations depending on the need to take into account linear, non-linear and rheological properties of soils [1].

The reliability and accuracy of the quantitative assessment of the stresses in the soil masses interacting with the underground part of the building largely depend on the choice of the geomechanical model of the massif and the design models of the soils comprising the massif in question [2].

It should be noted that the idea of limiting the computational domain in applied soil mechanics arose in the middle of the last century due to inconsistency of settlement results of foundations of structures considered by the elastic half-space model. Known are the models of N.A. Tsytovich, K.E. Egorov and others, limiting the thickness of compressible layer. There is known also the modern model limiting a computational domain both in depth and in width on the basis of which the analytical solution of a deflected mode of operation of such domain under the action of local loading in plane and spatial statement is received. Such limitation of calculation domain is caused by structural properties of strength and deformability of soils under volumetric changes and shape changes.

In order to describe the mechanical behaviour of media soils, it is possible to use several soil models in FEM [2–4]:

- linear model;
- non-linear elastic;
- Mora-Coulomb plastic model;
- The non-linear elastic-plastic Cam-glue model and the Cam-glue modification models;
- A non-linear elastic-plastic model of a Hardening soil.

The two-dimensional simulation of a bored micro pile is performed in the axisymmetric formulation of the problem, in which the pile is placed around the axis of symmetry, since in the axisymmetric formulation the lateral pressure must be the same [5–7].

The physical nature of FEM allows us to consider the "soils - pile foundation» system together. The stiffness of the foundation is defined by the description of its geometric dimensions, strength and deformation characteristics. Parameters of modelling of soil and pile foundation materials are given in Table 1.

Table 1 – Material properties of soil layers and piles

Parameters	Designation	Clay sand (brown) (EGE-1)	Silted sand (EGE-2)	Clay sand (red) (EGE-3)	Deep sand (EGE-5)	Clay sand (EGE-4)	Pile model
Material model	-	Coulomb- Mora	Coulomb- Mora	Coulomb- Mora	Coulomb- Mora	Coulom b-Mora	Linear- elastic
Ground behaviour	-	Drained	Drained	Drained	Drained	Drained	Non- porous
Weight in an unsaturated state	γ_{unsat}	16,7	18,8	19,8	17,6	17,0	24,0
Weight in water- saturated state	γ_{sat}	16,7	18,8	19,8	20,0	19,0	-
Young's module	E	9150	13000	13500	19000	20000	30000 00
Poisson's ratio	ν	0,3	0,3	0,3	0,3	0,33	0,3
Clutch	c	13	12	14	17	8	-
Angle of friction	φ	26	23	23	23	29	-

The geometric dimensions of the 500 mm wide and 31 m long pile model were used in the calculation.

A 15-node finite element mesh was automatically generated by Plaxis. In order to obtain a qualitative picture in the areas near the pile the finite element mesh was chopped up. After the element mesh was generated, the initial stress state from the self-weight of the soil was modelled. All displacements obtained during the initial stress-strain modelling phase were zeroed out before the probe plunge began. The calculation was carried out using a variable mesh with the Update Mesh option, implying the use of the so-called Updated Lagrange, where the finite element mesh is continuously updated during the calculation process [8].

The version of Plaxis used allows only a linear colour scale. Because of this, due to the large difference between the minimum and maximum shear strains, it turned out to be impossible to display them simultaneously in the same figure [9-10].

The calculations were carried out according to the finite element diagram shown in Figure 1.

Due to the symmetry of the pile foundation cross-section relative to the vertical axis, only half of the soil mass and pile foundation area were considered in the computational scheme and were automatically divided into triangular finite elements. The number of considered element types (layers) is 5 (the sequence of soil layers is shown in Figure 1).

The 31 m long piles were tested by means of a variety of simulations (Figure 1):

a) Model 1 – jack is installed inside at a depth of 1/2 pile – 15 m (method of Bi-Directional Static load test);

- b) Model 2 – jack is installed inside the pile at a depth of 29 m (method of Bi-Directional Static load test);
 c) Model 3 – jack is mounted on the pile head (method of Top down).

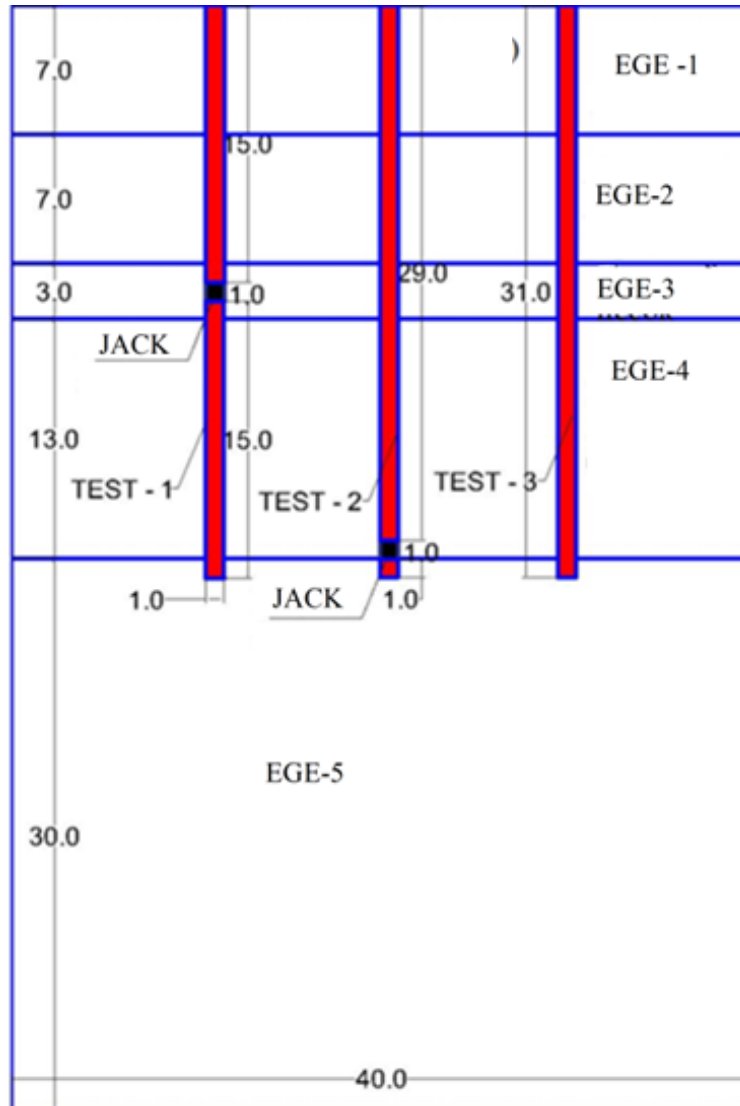


Figure 1 – Layout of the jacking arrangement of the pile or pile

2 Numerical simulation of pile testing of BDSLT and SLT methods (for models 1, 2 and 3)

This chapter deals with the first problem: calculating settlement of a pile foundation. The general methods for creating the geometric model, constructing the finite element mesh, performing the finite element calculation and evaluating the results are discussed in detail [6-11].

The load-bearing capacity of the piles was determined using the results of numerical modelling of the pile in the PLAXIS 2D software package. The stress-strain state of the foundation was calculated using the Moore-Coulomb elastic-plastic model. The calculations were performed in axisymmetric formulation [11–13].

The staged loading of the pile was simulated by increasing the applied load on the pile by 145 kN. The main parameters monitored for the results are the magnitude of the applied load and the pile settlement. As a result of the calculation, load-settlement plots of the pile are plotted [14].

Figure 2a, 2b and 2c show geometric models of a numerical simulation of a bored micro pile, including soil separation within a separately considered geotechnical element, a pile element

and a uniformly distributed micro pile load. The dimensions of the geometric model are taken from the condition that the stress distribution will be negligibly small within a given zone [15].

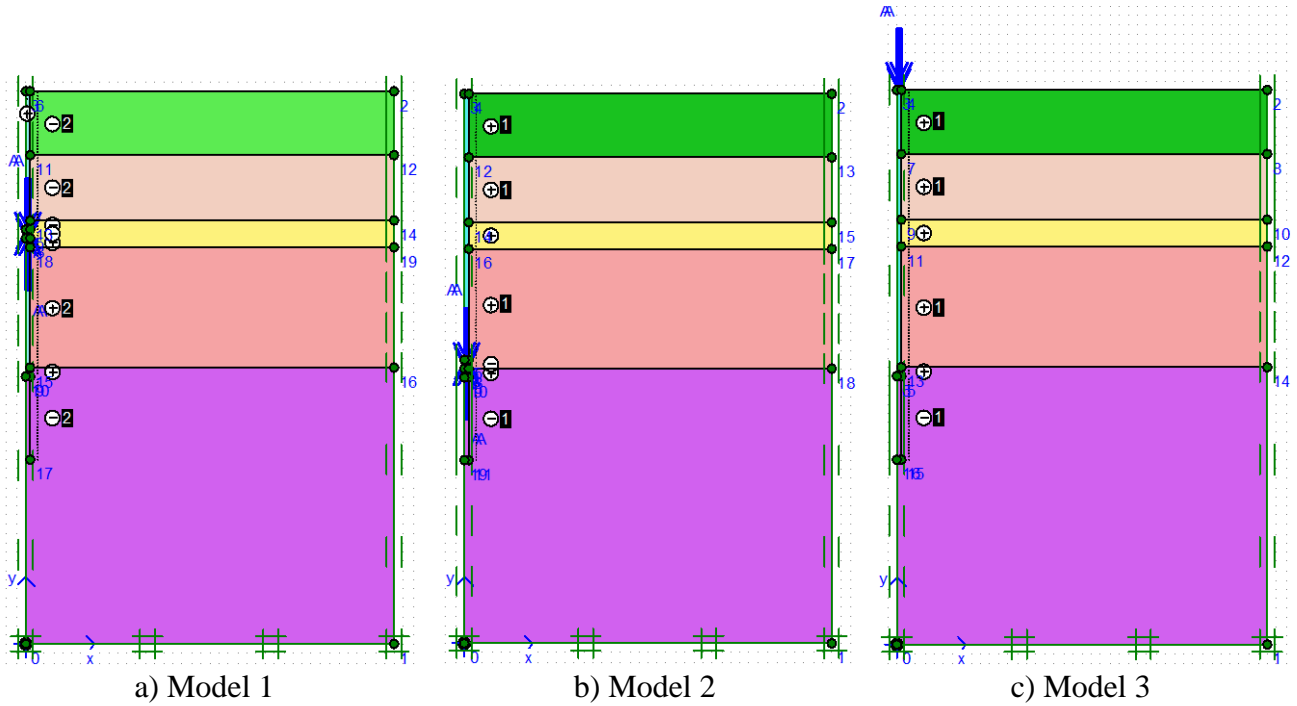


Figure 2 – Geometric model of a bored piles

Figure 3 show the finite element meshes generated automatically by the Plaxis software and represent a triangle system. Soil foundations and piles were modeled with 15-node finite elements. The construction method is based on the stable triangulation principle which is used to find the optimum mesh dimensions.

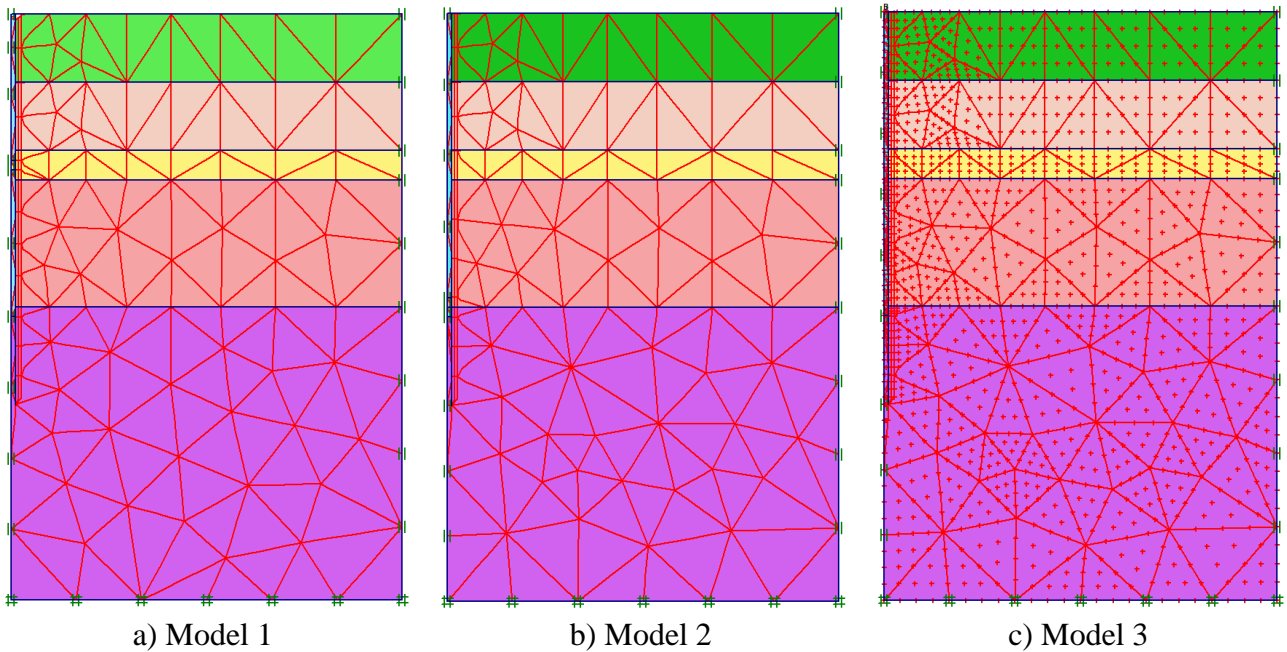


Figure 3 – Finite element grid: a - model 1, b - model 2 and c - model 3, respectively)

The calculation consists of six phases and will be set in Staged construction mode. Figure 4a, 4b and 4c show the deformed pile foundation meshes.

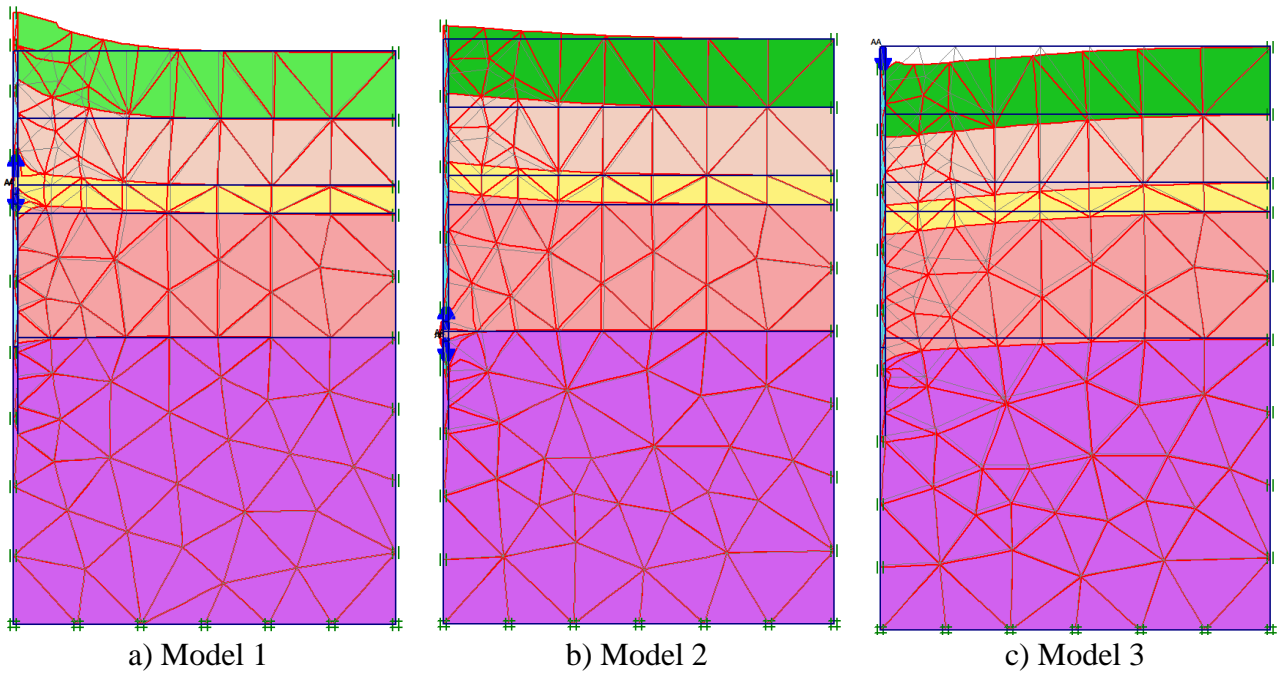


Figure 4 – Finite element mesh deformation

Figures 5, 6, 7 show isolines of total ground motions under static bidirectional and indentation loads for models 1, 2 and 3 respectively.

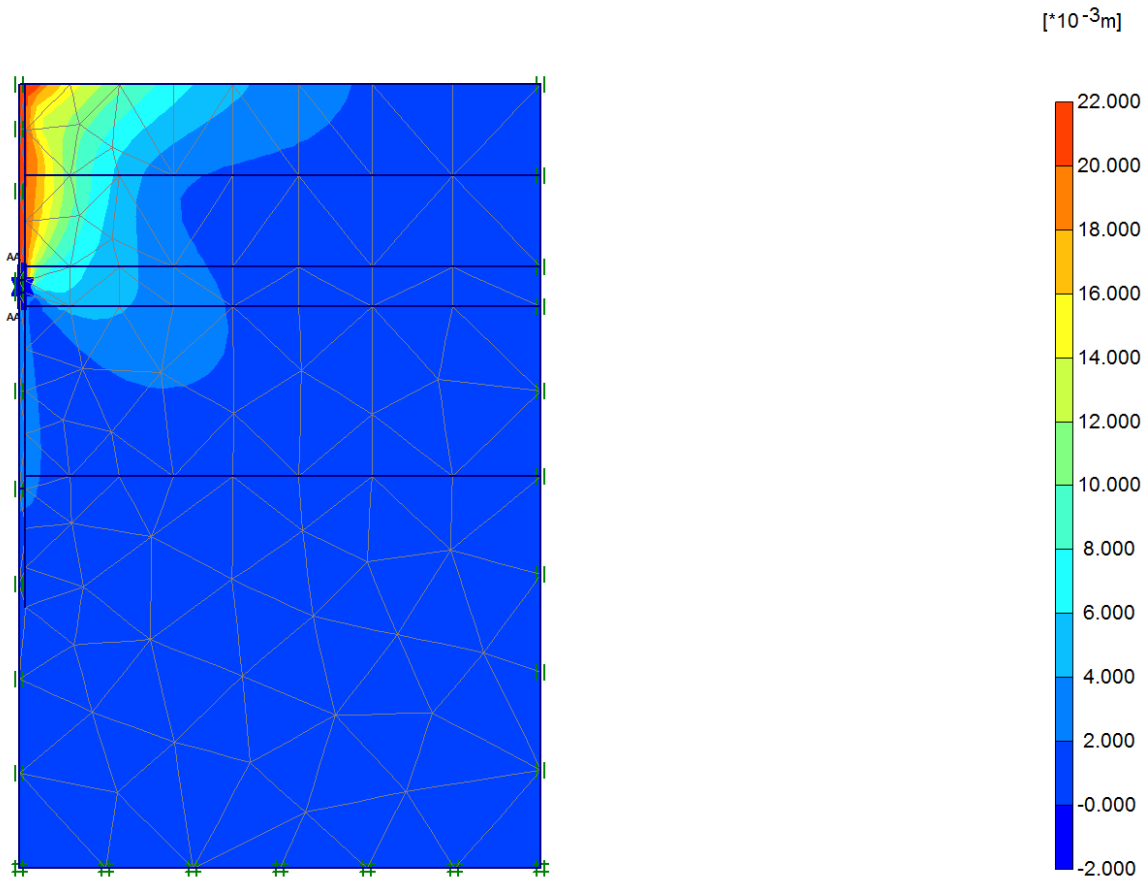


Figure 5 – Total settlement (model 1)

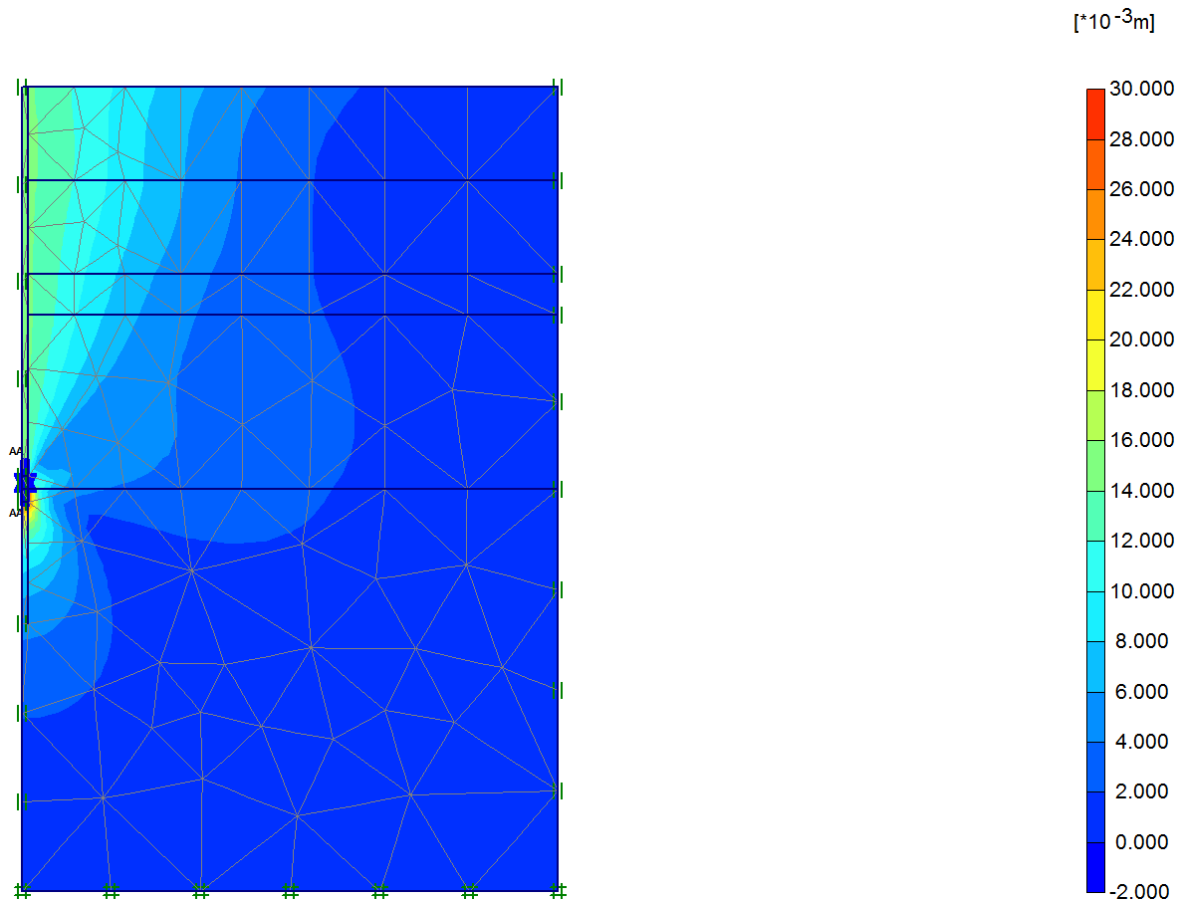


Figure 6 – Total settlement (model 2)

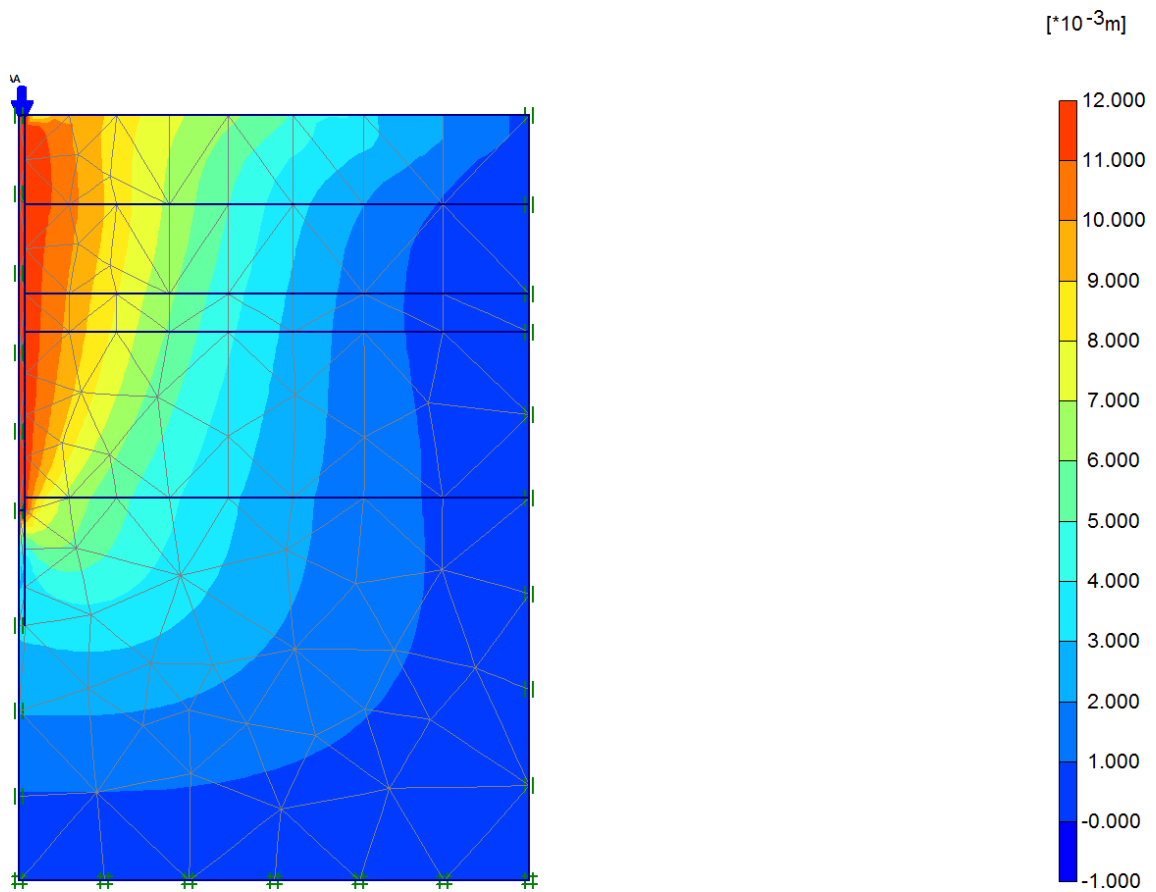


Figure 7 – Total settlement (model 3)

3. Results and Discussion

Based on the calculation results, displacements vs. bi-directional load plots are obtained (Figure 8).

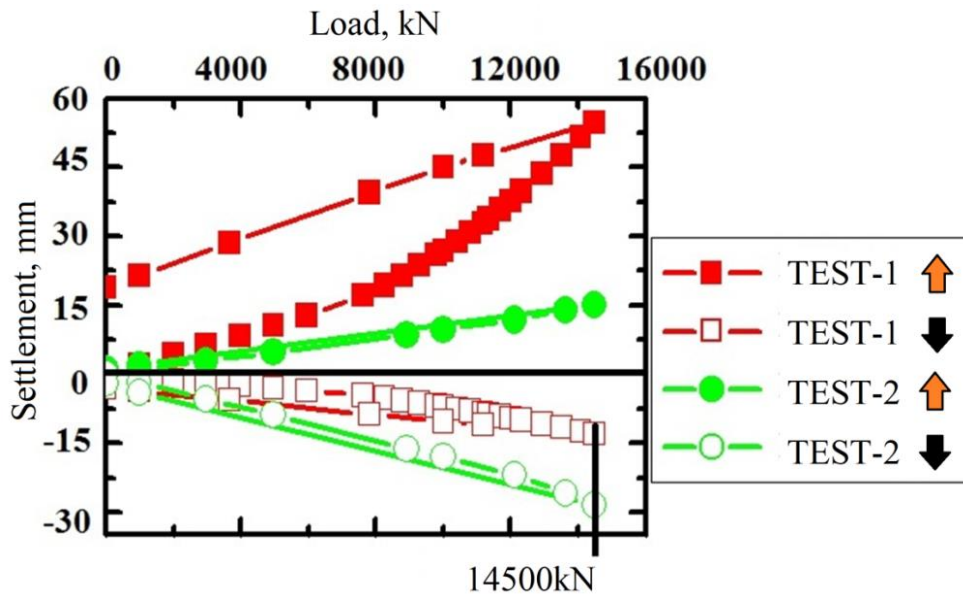


Figure 8 – Load-displacement test results (model 1 and 2, respectively)

Figure 9 shows a comparison of the numerical simulation test results: the load – settlement curve obtained by simulation 3 and the equivalent load – settlement curve of simulation 1 and 2.

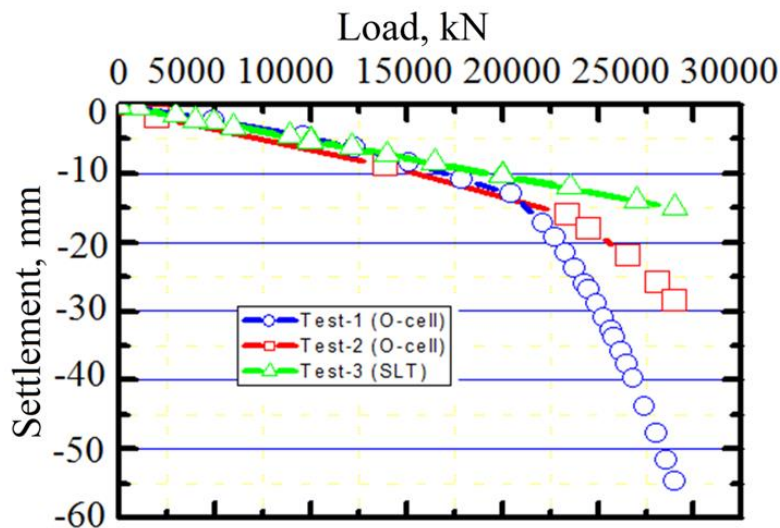


Figure 9 – Equivalent load-settlement curve and SLT test results (model 1, 2 and 3, respectively)

Overlapping of the curves showed that the convergence of the graphs is observed only in the initial stage of loading, further on the O-cell curve trajectory changes, which is characteristic of the creeping stage of ground resistance, whereas the SLT curve (in this stage of loading) is more characteristic of the elastic ground resistance.

Based on the results of the model 1 test, it was found that for a given load it was necessary to increase the jacking depth in the pile because the top test element had the lowest resistance on the side of the pile and consequently the actual ground load-bearing capacity of the pile was not determined.

Based on the results of model 2 testing, it was found that the given load and jacking depth in the pile meet the ground bearing capacity requirements of the pile. In this model it is possible to increase the jacking load until the pile reaches its full ground bearing capacity.

According to the results of the Model 3 test, the load is transferred from the jack to the pile body, and large stresses occur in the pile body. As can be seen in Figure 7, when the pile model is moved vertically, the highest stress is observed on the lateral surface and the lowest on the lower end of the pile, which is an indication of unequal load distribution.

4. Conclusions

1. The analysis of using axisymmetrical problem in elastoplastic statement by the finite element method for investigation of behaviour of the pile-to-base system has shown the expediency of using FEM implemented by the "Plaxis" software.

2. When testing the pile with hydraulic jacks and when segmenting it, special attention must be paid to studying the geotechnical structure of the soil mass at the site under investigation.

3. During the survey it is particularly important to identify possible zones of heterogeneity in the geological structure of the soils, such as areas of weathering, alternating soil layers, etc. These data have to be taken into account when testing with hydraulic jacks and dividing the pile into segments to obtain accurate design characteristics for a given soil layer.

4. When testing the soil with piles, in order to assess as accurately as possible the lateral friction and bearing capacity under the bottom end of the pile, a sound programme of load-bearing layer studies using laboratory and field tests as well as analysis of existing construction experience in these and similar soil conditions must be carried out.

Acknowledgments

This research has been funded by the Science Committee of the Ministry of Education and Science of the Republic of Kazakhstan (Grant No. AP13268718).

References

1. Analysis of Piled Raft Foundation on Soft Soil Using PLAXIS 2D / P.S. Wulandari, D. Tjandra // *Procedia Engineering*. — 2015. — Vol. 125. — P. 363–367. <https://doi.org/10.1016/j.proeng.2015.11.083>
2. Effect of Competent Caliche Layers on Measuring the Capacity of Axially Loaded Drilled Shafts Using the Osterberg Test / R. Afsharhasani, M. Karakouzian, V. Farhangi // *Applied Sciences*. — 2020. — Vol. 10, No. 18. — P. 6169. <https://doi.org/10.3390/app10186169>
3. The selection of soil models parameters in Plaxis 2D / O.V. Sokolova // *Magazine of Civil Engineering*. — 2014. — Vol. 48, No. 04. — P. 10–16. <https://doi.org/10.5862/MCE.48.2>
4. Elastic Analysis of Drilled Shaft Foundations in Soil Profiles with Intermediate Caliche Layers / M. Karakouzian, R. Afsharhasani, B. Kluzniak // *IFCEE 2015*. — San Antonio, Texas: American Society of Civil Engineers, 2015. — P. 922–928. <https://doi.org/10.1061/9780784479087.083>
5. Applications of PLAXIS 2D in the Calculation of Sheet Pile Wharf Structure / K. Xu, S. Zhang // *Advanced Materials Research*. — 2013. — Vol. 838–841. — P. 2223–2226. <https://doi.org/10.4028/www.scientific.net/AMR.838-841.2223>
6. Numerical Investigation into Lateral Behavior of Monopile Due to Scour Enhanced: Role of State-Dependent Dilatancy / N. Jia, J. Liu, X. Wang // *Applied Sciences*. — 2022. — Vol. 12, No. 2. — P. 921. <https://doi.org/10.3390/app12020921>
7. Influence of Groundwater Depth on Pile–Soil Mechanical Properties and Fractal Characteristics under Cyclic Loading / B. Yuan, Z. Li, W. Chen, J. Zhao, J. Lv, J. Song, X. Cao // *Fractal and Fractional*. — 2022. — Vol. 6, No. 4. — P. 198. <https://doi.org/10.3390/fractalfract6040198>
8. Fully Coupled Flow Deformation Analysis of Buried Concrete Pipe Using Finite Element Software PLAXIS 2D / T. Vickneswaran, V.S. Jella, N. Ravichandran, K.R. Piratla // *Geo-Extreme 2021*. — Savannah, Georgia: American Society of Civil Engineers, 2021. — P. 211–221. <https://doi.org/10.1061/9780784483695.021>
9. In-Situ Customization of the Helical Pile Design Procedure Using Plaxis 2D / A.G. Alekseev, S.G. Bezvoley // *Soil Mechanics and Foundation Engineering*. — 2020. — Vol. 57, No. 1. — P. 77–83. <https://doi.org/10.1007/s11204-020-09640-9>
10. Mathematical solution of the stone column effect on the load bearing capacity and settlement using numerical analysis / A. Madun, S.A. Meghzili, S. Tajudin, M.F. Yusof, M.H. Zainalabidin, A.A. Al-Gheethi, M.F.M. Dan,

- M.A.M. Ismail // Journal of Physics: Conference Series. — 2018. — Vol. 995. — P. 012036. <https://doi.org/10.1088/1742-6596/995/1/012036>
11. Settlements and Subgrade Reactions of Surface Raft Foundations Subjected to Vertically Uniform Load / D.-W. Chang, C.-W. Lu, Y.-J. Tu, S.-H. Cheng // Applied Sciences. — 2022. — Vol. 12, No. 11. — P. 5484. <https://doi.org/10.3390/app12115484>
 12. Site-specific soil reaction model for monopiles in soft clay based on laboratory element stress-strain curves / Y. Lai, L. Wang, Y. Zhang, Y. Hong // Ocean Engineering. — 2021. — Vol. 220. — P. 108437. <https://doi.org/10.1016/j.oceaneng.2020.108437>
 13. Influence of Vertical Load on the Lateral Response of Piles in Normally Consolidated and Over-Consolidated Clay: Centrifuge and Numerical Modelling / T. Liu, Y. Lai, B. He, N. Lv // Frontiers in Physics. — 2022. — Vol. 10. — P. 908181. <https://doi.org/10.3389/fphy.2022.908181>
 14. Bi-Directional Static Load Testing / A.Zh. Zhussupbekov, R.E. Lukpanov, A.R. Omarov // Geo-China 2016. — Shandong, China: American Society of Civil Engineers, 2016. — P. 35–42. <https://doi.org/10.1061/9780784480083.005>
 15. Experience in pile testing on different construction sites / A.S. Tulebekova, Ye. Ashkey, A.K. Zhankina // BULLETIN of L.N. Gumilyov Eurasian National University. Technical Science and Technology Series. — 2022. — Vol. 138, No. 1. — P. 76–82. <https://doi.org/10.32523/2616-7263-2022-138-1-76-82>

Information about authors:

Abdulla Omarov – PhD, Senior Lecturer, Department of Civil Engineering, L.N. Gumilyov Eurasian National University, Nur-Sultan, Kazakhstan, omarov_01@bk.ru
Gulshat Tleulnova – PhD, Acting Associate Professor, Department of Civil Engineering, L.N. Gumilyov Eurasian National University, Nur-Sultan, Kazakhstan, gulshattleulnova23@mail.ru

Author Contributions:

Abdulla Omarov – concept, methodology, resources, testing, editing, funding acquisition.
Gulshat Tleulnova – data collection, modeling, analysis, visualization, interpretation, drafting.

Received: 06.06.2022

Revised: 22.06.2022

Accepted: 23.06.2022

Published: 23.06.2022



Defects in a dilapidated building resulting in loss of bearing capacity of supporting structures

Alizhan Kazkeyev^{1,*}, Daniyar Kenzhebekov², Nursultan Tattikulov²

¹ Department of Civil Engineering, L.N. Gumilyov ENU, Nur-Sultan, Kazakhstan

²NTDK Group LLP, Nur-Sultan, Kazakhstan

*Correspondence: alizhan7sk@gmail.com

Abstract. This article is devoted to assessing the effectiveness of technical inspection of the condition and the degree of influence of various factors on the reliability of buildings. Technical inspection of the condition of buildings and structures is an important procedure for making decisions about the suitability of the structure for its further operation. Technical inspection should be carried out by specialized accredited organizations that have the necessary expertise and equipment. Adverse environmental factors, poor quality of construction and installation work and general physical deterioration of the building have a direct impact on the safety of people staying in it. The object of the survey was the building of a secondary school in the Karaganda region. Visual and instrumental inspection was carried out at the object, including determination of technical condition and damage categories by shock-pulse method and geodetic surveying. According to the results of the inspection of the object the conclusion of improper condition of the load-bearing structures belonging to category IV, i.e., pre-emergency state of the structures was assigned.

Keywords: technical inspection, nondestructive methods, defects, tolerance, supporting structures.

1. Introduction

Technical inspection of buildings - an important procedure by which to decide the fate of the structure [1]. By definition, technical inspection is a complex of measures to determine and assess the actual values of controlled parameters that characterize the operational condition, suitability, performance and energy efficiency of buildings and structures to determine the possibility of further operation or the need for structural intervention [2]. In the territory of the Republic of Kazakhstan, the survey should be carried out by an organization accredited for such activities [3]. Classically, the inspection consists of the following steps [4]: 1) Preparatory, which is the study of the original documentation (design and construction documents, architectural and planning decisions, technical specifications, materials on planned repair, previous calculations of supporting structures, etc.), and the contract between the customer and the contractor works; 2) Visual inspection, which checks compliance between the actual geometry of the structure with the available schematic construction drawings; 3) Instrumental examination, which assess the technical condition and set up a technical inspection of the building; 4) Technical inspection, which reveals the differences in the technical condition of the building and the state of its elements. An "instrumental examination" finds out the differences between the actual value of any technical condition and the "tolerances" specified in the standards [5]. A variety of tools and methods of destructive and nondestructive testing are used during the survey [6].

Most often technical inspection is carried out for social facilities that are on the balance sheet of public institutions [4]. These are objects such as schools, kindergartens, libraries, museums, and the like. The object of the survey in this study is the building of the municipal state institution

"Amangeldy comprehensive school" in Karaganda region, Kazakhstan. The design and construction of the school began in 2003, and the school opened to students in 2007. Inspections at the site were carried out in 2017 and 2022. The peculiarity of this case is that the school building was in a mothballed state from the start of construction until it was put into operation. In this example, we can clearly assess the impact of natural factors on the integrity of the building when no measures are taken to maintain the current condition of the building. The most recent survey revealed the building to be unsuitable for further operation for a number of reasons [5]. This article examines the features of the load-bearing structures of the school building that are subject to significant damage and are on the verge of collapse (foundation, walls, floors, and coverings).

2. Methods

The object of the survey (school) is two-story and consists of 3 adjacent blocks, two of which contain an auditorium fund, and the last block is a gymnasium. According to the project documentation, the foundation of the object is strip foundation made of precast reinforced concrete blocks. Walls of the main part are 0.57 m thick big-block ones, and those of the gym are brick ones. The ceilings and coverings of the main part are made of multi-hollow reinforced concrete slabs, and the cover of the gym - of ribbed reinforced concrete slabs.

The expert inspection of the building structures was performed in accordance with [5] and consisted of three stages:

- Preparatory (collection and study of initial materials);
- Visual (inspection and photo-fixation of defects, establishing their nature and extent) and instrumental (establishment of the technical condition and determination of damage categories by shock-pulse method and geodetic survey) examination of the building;
- Drawing up a technical report.

Pits were made at 5 points (Figure 1) in order to inspect the condition of the foundations, to determine their depth and to check their strength.

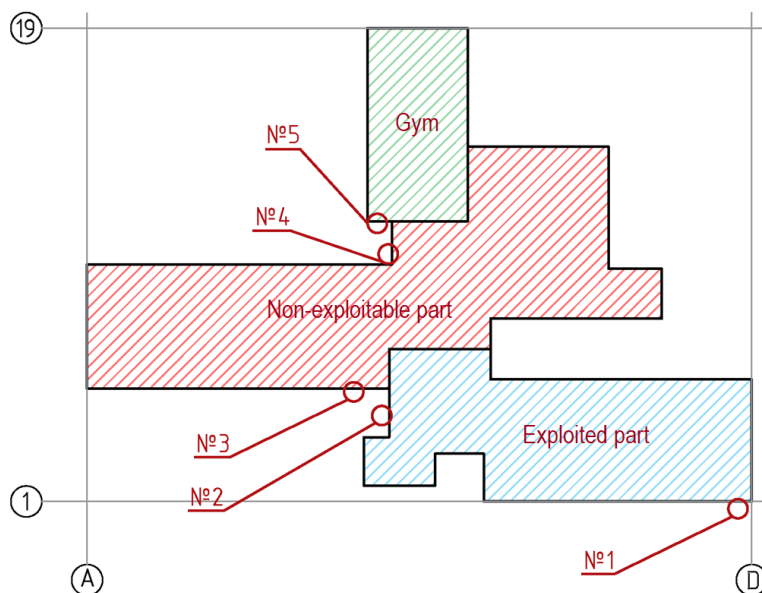


Figure 1 – Pits layout

3. Results and Discussion

3.1 Foundation

Visual and instrumental examination of the building foundation revealed that the foundation is strip foundation of precast reinforced concrete blocks on a concrete pad with crushed stone

preparation. According to the results of pits, the depth of foundation from ground level is from 2.95 m to 3.25 m, depending on the absolute ground level mark. At the time of visual and instrumental inspection of the building's foundation, there were ubiquitous traces of efflorescence on the walls of the foundation blocks, local shrinkage cracks in the body of the foundation blocks (Figure 2).



Figure 2 – Efflorescence (left) and shrinkage cracks (right) of foundation

Shock-pulse tests revealed concrete strength values of foundation blocks from 33.9 to 40.3 MPa, with an average of 37.8 MPa.

The overall technical condition of the foundation is satisfactory. The category of assessment of the technical condition of the foundation is Category II (serviceable structure). According to [5] and the identified defects, the physical deterioration of the foundation is 39%. These figures are atypical for a building less than 20 years old, but it is worth bearing in mind that the building was exposed to a hostile environment prior to commissioning. For example, the degree of physical deterioration for buildings less than 20 years old is usually about 10% with proper maintenance [7].

3.2 Walls

The walls of the main part of the building are made of large expanded clay concrete blocks with a thickness of 570 mm. The walls of the gymnasium are made of 380 mm thick brickwork and 120 mm thick cladding. The technical inspection revealed that the walls of part of the gymnasium were re-built from brickwork. The brickwork of the walls of the gymnasium was not performed with high quality, there were no reinforcing belts, the new masonry was not bound to the old masonry, and vertical deviations were visually observed. During construction and installation works of the walls of the gymnasium concrete blocks of different sizes were partially used instead of bricks, which had an adverse effect on the wall structure in the form of uneven load. For this reason, cracks occurred in the wall body (Figure 3, left). To mount the reinforced concrete beams, brick columns were made in the body of the gymnasium's load-bearing walls 630 mm wide. The brick columns were reinforced with metal casing made of angles, but the reinforcement structures are not of good quality and do not ensure their performance (Figure 3, right).



Figure 3 – Weak bonding (left) and poor strengthening (right) of masonry

According to the geodetic surveys of the gymnasium walls, the average value of vertical deviation from the plane was 80-90 mm, and the maximum deviation was 147 mm. While the allowable deviation per floor is 10 mm according to [5]. The inspection of the wall blocks in the unexploited part of the building revealed that under the influence of natural conditions there was a gradual destruction and delamination of the wall blocks. At the time of the visual and instrumental examination of the building walls a number of defects were revealed. Schemes of their location are shown in Figure 4 below.

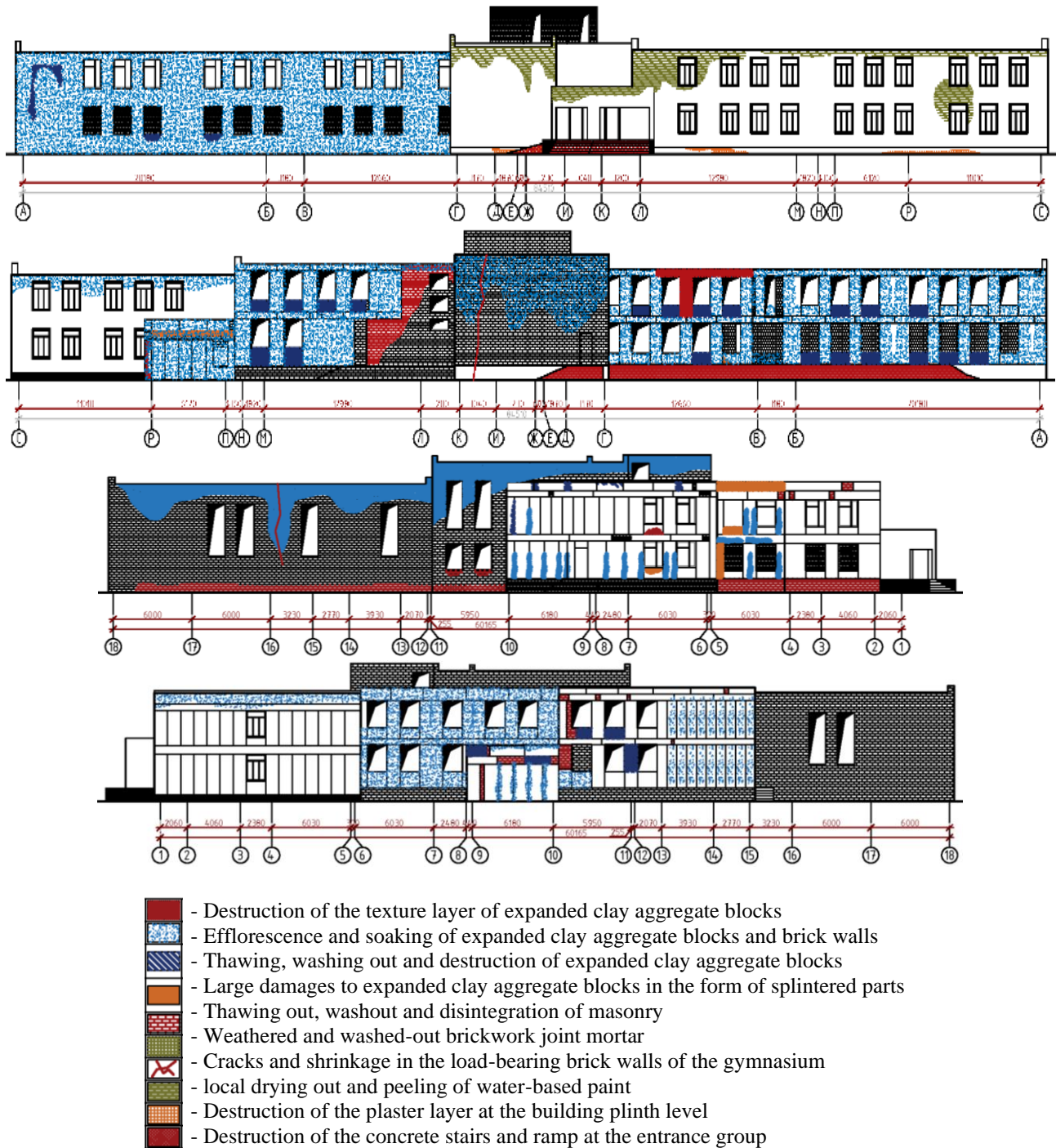


Figure 4 – Defects of walls

General technical condition of the walls - unsatisfactory. Evaluation category of the technical condition of the walls - Category IV (pre-emergency condition of the structure). According to [5] and the defects detected, the physical deterioration of the walls is 65%.

3.3 Floor and cover slabs

The inspection revealed that the floor and roof slabs in the main part of the building are prefabricated hollow reinforced concrete, the gym floor slabs are prefabricated hollow reinforced concrete, and the gym floor slabs are prefabricated ribbed reinforced concrete.

According to the results of visual and instrumental examination of the floor and ceiling slabs, various defects were identified. The scheme of their location is shown in Figure 5 below.

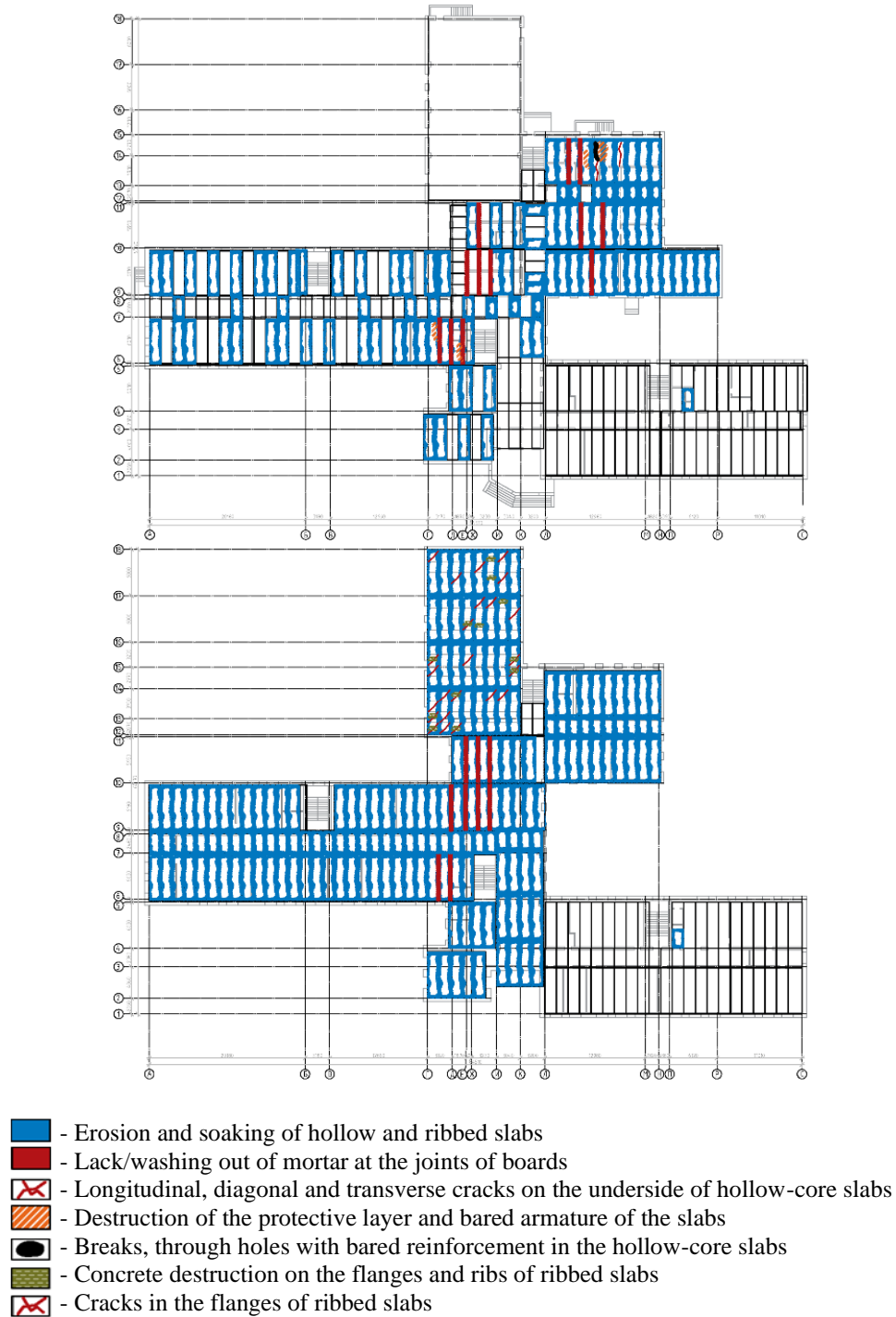


Figure 5 – Defects of floor and cover slabs

Cracks in the longitudinal, transverse ribs and slab flange occurred as a result of soaking of the slabs due to leaking roofing and environmental exposure. Corrosion of the reinforcement is usually observed in places with low density and insufficient thickness of the protective layer of

concrete. The corrosion products of the reinforcement, having a greater volume, have a spreading action and gradually destroy the concrete of the protective layer, leading to the formation of cracks. Through these cracks the moisture comes most intensively, accelerating the process of corrosion of the reinforcement and increasing the width of the crack opening. Subsequently, these processes lead to crumbling of the concrete protective layer, bare reinforcement and its intense corrosion.

According to the geodetic survey of the gymnasium floor slabs, the average deflection of the slabs is 18-20 mm, the maximum deflection is 29 mm. The allowable value of the deflection of the plates is 30 mm. Tests by shock impulse method revealed concrete strength values of foundation blocks from 26.8 to 31.9 MPa, with an average of 29.4 MPa.

Also, at the time of visual and instrumental inspection, an emergency section of the basement floor slab under the gymnasium was revealed - an area of a broken multi-hollow slab (Figure 6, left). Also areas of the slabs with unacceptable deflection and diagonal cracks were revealed. These floor slabs cannot be restored. In the classrooms in the operational part of the building, there is a displacement of up to 50 mm from the vertical of the slabs (Figure 6, right).



Figure 6 – Breaks (left) and displacement (right) of slabs

The general technical condition of the floor and roof slabs is unsatisfactory. Evaluation category of the technical condition of the floor slabs - Category III (limited serviceability of the structure). According to [5] and the defects detected, the physical deterioration of the floor and cover slabs is 55%.

4. Conclusions

The inspected building has a large number of defects on the non-exploited part of the building, as for many years it stood under the direct influence of natural conditions, which negatively affected the load-bearing structures. For example, the average vertical deviation of the walls of the gymnasium from the plane was 90 mm, which is 9 times the allowable deviation of 10 mm per floor. Also, according to the visual-instrumental survey and geodetic surveys, we can conclude that the construction and installation work on the erection of the part of the gymnasium was performed poorly. There are complex problems with the building structures related to physical deterioration. Due to the incomplete construction of the building, structural materials begin to lose their mechanical properties. For example, during the years of downtime, the physical deterioration of the walls of the school due to weather conditions was 65%, making it impossible to continue operating the building.

According to the results of the expert examination and evaluation, it can be concluded that at the time of the survey according to the category of assessment of the technical condition, supporting structures of the school building refers to Category IV (pre-emergency condition of structures).

The methods of interpreting the results of technical inspection are recommended to be used for similar case studies.

Acknowledgments

The data for current study was retrieved from NTDK Group LLP (Nur-Sultan, Kazakhstan).

References

1. Building Inspection System for Evaluating the Technical Performance of Existing Buildings / R. Bortolini, N. Forcada // Journal of Performance of Constructed Facilities. — 2018. — Vol. 32, No. 5. — P. 04018073. [https://doi.org/10.1061/\(ASCE\)CF.1943-5509.0001220](https://doi.org/10.1061/(ASCE)CF.1943-5509.0001220)
2. Assessment of heritage timber structures: Review of standards, guidelines and procedures / M. Riggio, D. D'Ayala, M.A. Parisi, C. Tardini // Journal of Cultural Heritage. — 2018. — Vol. 31. — P. 220–235. <https://doi.org/10.1016/j.culher.2017.11.007>
3. Building Information Model (BIM) Implementation in Perspective of Kazakhstan: Opportunities and Barriers / D. Aitbayeva, M. Hossan — 2020. — Vol. 14. — P. 13–24. <https://doi.org/10.9734/JERR/2020/v14i117113>
4. Analysis of methods for assessing the condition of surveyed facilities in Taraz City / A. Kazkeyev, A. Aniskin // Technobius. — 2022. — Vol. 2, No. 1. — C. 0015. <https://doi.org/10.54355/tbus/2.1.2022.0015>
5. SP RK 1.04-101-2012. «Survey and assessment of the technical status of buildings and constructions» [Electronic resource] // PARAGRAPH information system. — Access mode: https://online.zakon.kz/Document/?doc_id=39108718 (access date: 27.05.2022).
6. On traditional and modern methods and devices for controlling the strength of concrete / Y.B. Utepov, A.B. Kazkeyev // Herald of the Kazakh-British technical university. — 2021. — Vol. 16, No. 4. — P. 193–199.
7. Information support of monitoring of technical condition of buildings in construction risk area / M.E. Skachkova, O.Y. Lepihina, V.V. Ignatova // Journal of Physics: Conference Series. — 2018. — Vol. 1015. — P. 042056. <https://doi.org/10.1088/1742-6596/1015/4/042056>

Information about authors:

Alizhan Kazkeyev – PhD Student, Department of Civil Engineering, L.N. Gumilyov Eurasian National University, Nur-Sultan, Kazakhstan, alizhan7sk@gmail.com

Daniyar Kenzhebekov – MSc, Expert on technical inspection of buildings and structures, NTDK Group LLP, Nur-Sultan, Kazakhstan, daniyar.ken@gmail.com

Nursultan Tattikulov – MSc, Expert on technical inspection of buildings and structures, NTDK Group LLP, Nur-Sultan, Kazakhstan, tn_expert@mail.ru

Author Contributions:

Alizhan Kazkeyev – concept, methodology, visualization, interpretation, drafting, editing.

Daniyar Kenzhebekov – resources, testing, analysis.

Nursultan Tattikulov – data collection, modeling, funding acquisition.

Received: 01.06.2022

Revised: 27.06.2022

Accepted: 27.06.2022

Published: 27.06.2022



On-site pilot testing of maturity sensors in conjunction with ambient condition monitoring device to get an insight into the concrete strength gain process

Yelbek Utepov^{1,2}, Shyngys Zharassov^{1,*}

¹ Department of Civil Engineering, L.N. Gumilyov Eurasian National University, Nur-Sultan, Kazakhstan

²CSI Research&Lab, LLP, Nur-Sultan, Kazakhstan

*Correspondence: zhshzh95@gmail.com

Abstract. The article demonstrates the performance of newly developed concrete maturity sensors on the construction site of residential complex “New Line” in Nur-Sultan. The sensors were mounted on the rebar of reinforced concrete structures to monitor the curing temperature of poured concrete grade M350 during 7 days. Additionally, the sensor device monitoring ambient temperature and relative humidity was set nearby. 14 cubic specimens were molded for compression test to determine the concrete strength. To get an idea on the degrees of influence of considered factors on concrete strength gain, the correlation analysis was conducted. As expected, the curing temperature showed a significant correlation with compressive strength, and its degree of influence amounted 58%. The ambient temperature with influence degree of 36% seemed to affect the concrete strength vividly. The relative humidity affected insignificantly with 6%. Based on conducted investigations the well-enough performance of maturity sensors is concluded. Moreover, there was set plans on the extension of their software solution with colored cross-correlation analysis technique.

Keywords: maturity sensor, construction site, cross-correlation analysis, concrete strength, internal and external factors.

1. Introduction

Monitoring the influence of internal and ambient factors is an important step when constructing a monolithic building frame, especially at early ages of concrete curing. As is known, the cement hydration in the concrete mix is accompanied by the heat release. Sometimes, depending on the composition and type of concrete as well as the massiveness of a structure, the internal temperature during exothermal process of concrete hardening may reach 90 °C. In majority of cases the dynamics of curing temperature may be describes with a sharp increase at the first few days after pouring, continued by general declining trend with slight fluctuations. Observation of such external factors as ambient temperature and relative humidity may give a certain understanding on the concrete hardening process as well. The external temperature may effect on the curing temperature unfavorably by cooling it. And the relative humidity at the surrounding air may somehow either extend the designed water content in the concrete or reduce it to a certain level interfering with the process of cement hydration [1]. Therefore, real time monitoring of these factors can potentially prevent undesirable consequences with concrete curing process. Previous studies show much of the examples of how these factors may be monitored on site using various sensor devices. One of the most popular devices to monitor internal temperature is a maturity sensor [2]. As of now, different types of maturity sensors have been invented, including embedded ones. Main purpose of the maturity sensors is to help estimating a concrete strength by indirect methods using a certain relationship between the temperature-time factor and strength, which was described in some international standards [3]. This relationship has been thoroughly discussed in previous studies [4], as well as some its modifications were presented. The sensors monitoring ambient conditions also exist and developed

in different variations [5]. One common thing that has to be taken into account on the sensors monitoring all the factors affecting certain characteristics of a building structure is a simultaneity of measurements. This must be always set precisely to make fair assumptions on the effect of factors on the concrete strength. In the sensor devices developed during the studies of [6] and [7] the aspect of simultaneity is reached by setting a specific measurement interval programmed to their Arduino microcontrollers in advance. By this moment these sensor devices were tested only on small precast structures, and fulfilled the expectations. However, they were not yet tested on site, on the structures of a monolithic building frame. Therefore, this study is aimed on pilot testing of the newly developed sensor devices as well as monitoring internal and ambient conditions affecting the strength of concrete in the massif structures on site.

2. Methods

The pilot test of sensor devices was held on the construction site of residential complex “New Line” in the city of Nur-Sultan, Kazakhstan. One maturity sensor was installed on the rebar of a raft foundation and another one on the rebar of pillar as shown in Figure 1 below, and the sensor device monitoring ambient conditions was put nearby. The measurement interval was set to 1 hour. So that each hour one reading was obtained.

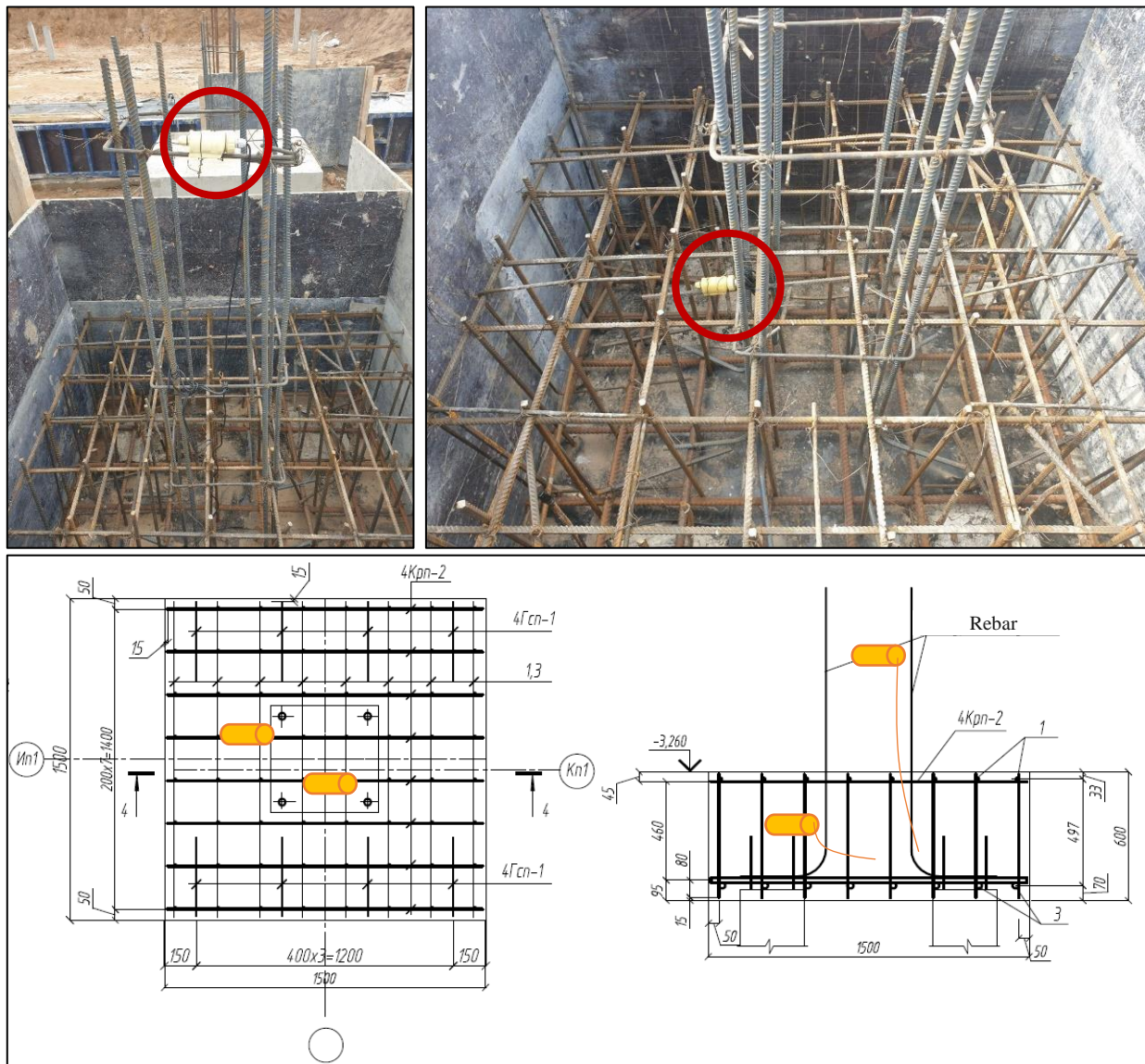


Figure 1 – Maturity sensors installed on rebar

Before pouring a concrete mix grade M350 on the formwork, 14 cubic specimens were sampled to monitor the compressive strength of the concrete of the structures. The monitoring was conducted over one week. The compression tests (Figure 2) were conducted each day on 2 cubic specimens according to [8]. The compressive strength values were averaged for each day.

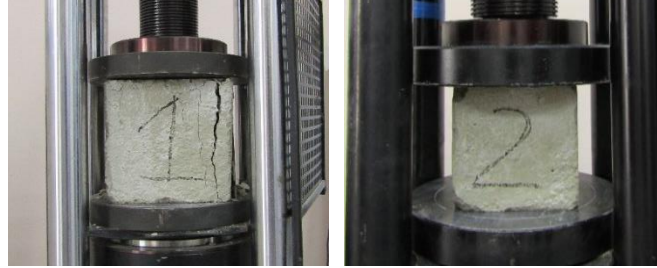


Figure 2 – Compression test of concrete specimens

At the end of a week the collected measurement data and compression test results were processed and analyzed on Excel. The correlation analysis was conducted to investigate the influence of internal temperature, ambient temperature and relative humidity on the concrete strength gain using classical Equation 1 below:

$$r_{i,a} = \frac{\sum_{a=1}^7 (F_i - \bar{F}_i) \cdot (R - \bar{R})}{\sqrt{\sum_{a=1}^7 (F_i - \bar{F}_i)^2 \cdot \sum_{a=1}^7 (R - \bar{R})^2}}, \quad (1)$$

where: i – considered factors: curing temperature (°C), ambient temperature (°C), and relative humidity (%).

a – curing age (day); in current case we considered first 7 days;

F_i and \bar{F}_i – i factor and its average value for age a respectively;

R and \bar{R} – strength (MPa) and its average value for age a respectively.

The degrees of influence of considered factors on concrete strength gain was obtained on via weighting of the modulus of correlation coefficients, so that the sum of obtained values equals one.

3. Results and Discussion

Figures 3 below shows the results of monitoring curing temperature of concrete in the raft foundation and the pillar. Because both structures were poured with concrete mix simultaneously, for the further analysis the average of temperature values from both maturity sensors were taken.

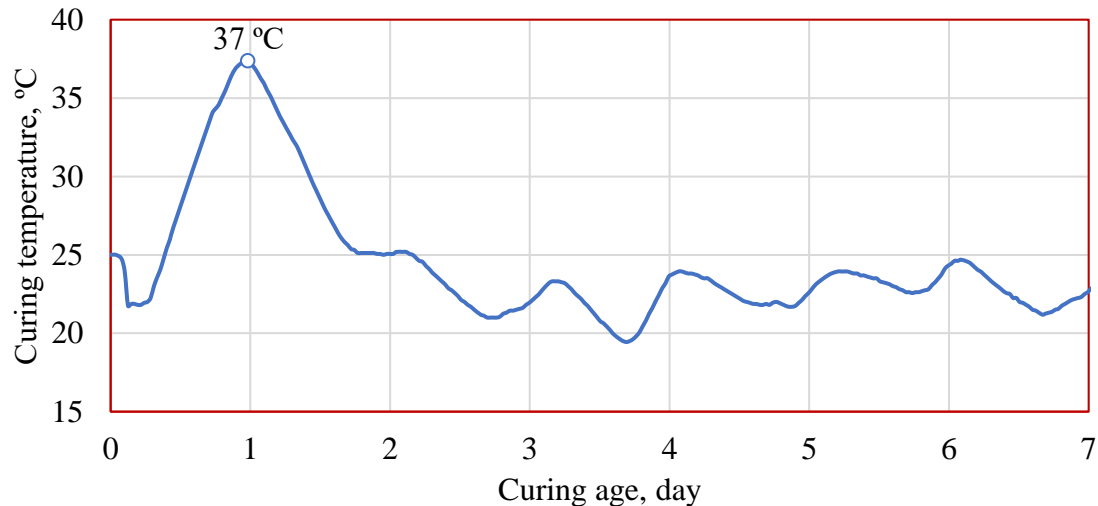


Figure 3 – Internal temperature monitoring results

As is seen from the chart above, the cement setting started 6 hours after pouring the concrete mixture in the structures. Since then, the curing temperature started dramatically rising up to 37 °C, keeping this level for around 3 hours. Then it dropped sharply, and started fluctuating within the range from 20 to 25 °C. The fluctuation may be explained with the difference of ambient conditions between day-time and night-time, which is shown in the Figure 4 below.

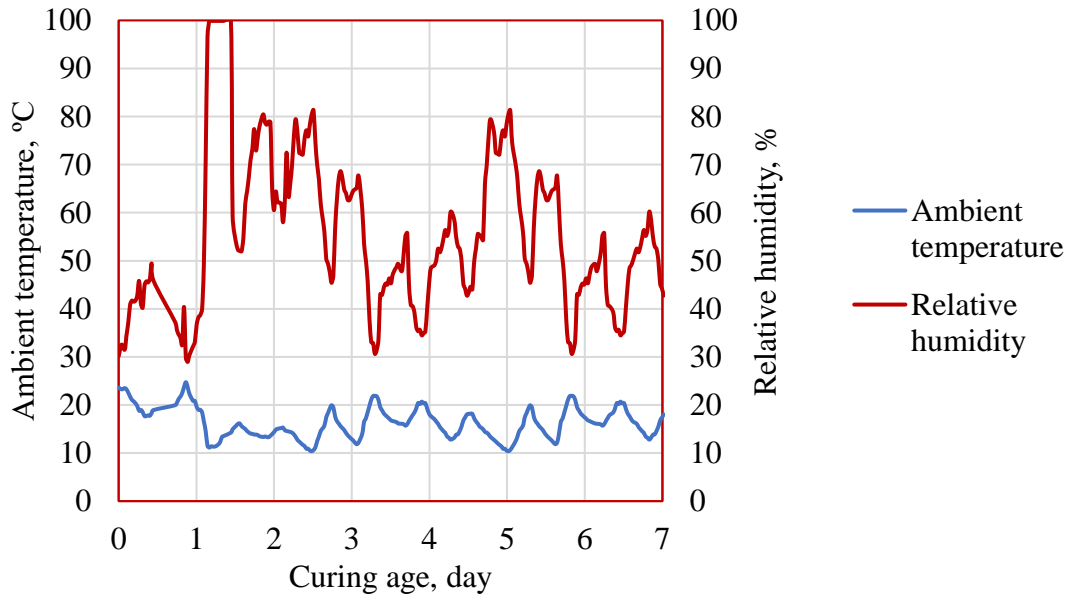


Figure 4 – Ambient conditions monitoring results

From the charts of ambient temperature and relative humidity over 7 days period can be observed that their general trend somehow coincides with those of curing temperature. Another clear trend is that when the ambient temperature is rising, the relative humidity is dropping, as vice-versa. In general, during the monitoring period the temperature outside was ranging between 10 to 25 °C. The relative humidity of the air at those days was ranging from 29 to 100 %.

The results of compression test of cubic specimens are shown in Figure 5 below. The values of compressive strength presented are those of average between two specimens for each curing day.

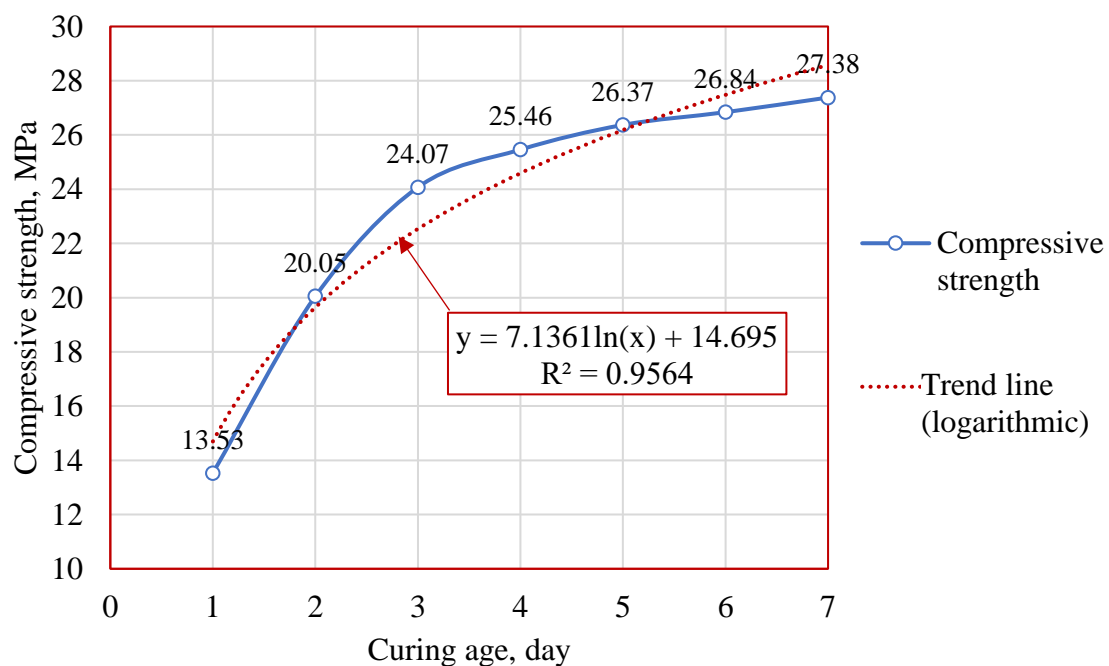


Figure 5 – Compression test results

From the chart above we can observe that over 7 days the concrete gained the strength of more than 27 MPa. This is more than 70% of the projected strength of concrete grade M350. It is seen that the first 3 days the strength is gaining faster than that of following days. In order to conduct correlation analysis, it was necessary to retrieve the hourly strength values. Therefore, the trend line and the strength function were extracted from the existing values for each of 7 days. It was decided to use the logarithmic function describing the trend of concrete strength gain due to for this case it had a highest coefficient of determination ($R^2 = 0.9564$). Further, using the Equation 1 above, the correlation analysis was conducted between all the considered factors and compressive strength (Table 1).

Table 1 – Cross-correlation analysis

	Compressive strength	Curing temperature	Ambient temperature	Relative Humidity
Compressive strength		-0.465	-0.286	0.046
Internal temperature	-0.465		0.115	0.105
Ambient temperature	-0.286	0.115		-0.872
Relative Humidity	0.046	0.105	-0.872	
Degrees of influence on strength gain:		58%	36%	6%

The cross-correlation above presented in green and blue colors demonstrate clear picture of how significant or insignificant of correlation between considered parameters. From market green cells is seen that the compressive strength has a high correlation with curing temperature; next is ambient temperature, and relative humidity. This is obvious, since the curing process releases a heat and the more the temperature the faster the strength gain. It can be also observed that the ambient temperature and relative humidity are strongly correlated. This proves the trend discussed above. The last line in the table shows the estimates of the degrees of influence of various considered factors on the concrete strength gain; the cells are marked blue. They were estimated taking the weighted modulus of each correlation coefficient. Thus, it can be seen that the curing temperature like always influenced greater than that of other factors. However, 36% of influence degree in this study is taken by ambient temperature. The relative humidity played insignificant role in the strength gain process.

The obtained results clearly show how demonstratively the strength gain process can be presented and used when monitoring the concrete structures. Previous studies [5-6] somewhat have something similar, however the cross-correlation technique in this study seems easier to understand. Moreover, the non-volatile manner of proposed estimations may be straightforwardly integrated to a computer or mobile software for monitoring purposes.

4. Conclusions

This study demonstrated on the basis of sensor devices and compression tests an easy-to-use technique for monitoring the concrete strength gain process, as well as on fly presentation of how various factors may affect it. The proposed technique is replicable and integrable to various computer or mobile programs.

The pilot test where the newly developed sensor devices were used disclosed fairly well performance of the latter. Therefore, it is planned to extend its software with the functionality to visualize the real-time cross-correlation between the internal and ambient factors, and concrete strength values. This may give opportunity to potential users for making better decisions during treatment of freshly poured concrete, as well as its hardening process.

Acknowledgments

This research was funded by the Science Committee of the Ministry of Education and Science of the Republic of Kazakhstan (Grant № AP08052033).

Personnel of New Line Project LLP are acknowledged for providing access on the construction site to make pilot tests.

References

1. Factors affecting the compressive strength of the concrete [Electronic resource] / Civilengineeringbible // CivilEngineeringBible.com. — [2022]. — Mode of access: <https://civilengineeringbible.com/article.php?i=275> (accessed date: 01.06.2022).
2. Monitoring concrete compressive strength using IoT-based wireless sensor network / N. Ha, H.-S. Kim, H.-S. Lee, S. Lee // 2021 IEEE International Conference on Consumer Electronics-Asia (ICCE-Asia). — Gangwon, Korea, Republic of: IEEE, 2021. — P. 1–3. <https://doi.org/10.1109/ICCE-Asia53811.2021.9641999>
3. Use of maturity method to estimate early age compressive strength of slab in cold weather / B.H. Tekle, S. Al-Deen, M. Anwar-Us-Saadat, N. Willans, Y. Zhang, C.K. Lee // Structural Concrete. — 2022. — Vol. 23, No. 2. — P. 1176–1190. <https://doi.org/10.1002/suco.202000693>
4. Complex Maturity Method for Estimating the Concrete Strength Based on Curing Temperature, Ambient Temperature and Relative Humidity / Y. Utepov, A. Aniskin, A. Tulebekova, A. Aldungarova, S. Zharassov, A. Sarsembayeva // Applied Sciences. — 2021. — Vol. 11, No. 16. — P. 7712. <https://doi.org/10.3390/app11167712>
5. Assembling a multisensory device for monitoring and assessing concrete curing conditions / Ye.B. Utepov, T.A. Tolkyrbayev, A. Aniskin, S.B. Akhazhanov, Sh.Zh. Zharassov, A.S. Tulebekova, M.S. Akishev // Eurasian Physical Technical Journal. — 2022. — Vol. 19, No. 1. — P. 90–98. <https://doi.org/10.31489/2022No1/90-98>
6. Prototyping an embedded wireless sensor for monitoring reinforced concrete structures / Ye.B. Utepov, O.A. Khudaibergenov, Ye.B. Kabdush, A.B. Kazkeev // Computers and Concrete. — 2019. — Vol. 24, No. 2. — P. 95–102. <https://doi.org/10.12989/cac.2019.24.2.095>
7. Effect of the shape and structure of maturity sensor's plastic housing on its physico-mechanical properties / Ye.B. Utepov, S.B. Akhazhanov, A. Aniskin, Sh.Zh. Zharassov // Eurasian Physical Technical Journal. — 2021. — Vol. 18, No. 3(37). — C. 83–87. <https://doi.org/10.31489/2021No3/83-87>
8. GOST 10180 Concretes. Methods for strength determination using reference specimens. — 2012.

Information about authors:

Yelbek Utepov – PhD, Associate Professor, Department of Civil Engineering, L.N. Gumilyov Eurasian National University, Nur-Sultan, Kazakhstan, utepov-elbek@mail.ru

Shyngys Zharassov – PhD Student, Department of Civil Engineering, L.N. Gumilyov Eurasian National University, Nur-Sultan, Kazakhstan, zhshzh95@gmail.com

Author Contributions:

Yelbek Utepov – concept, methodology, resources, interpretation, editing, funding acquisition.

Shyngys Zharassov – data collection, testing, modeling, analysis, drafting, visualization.

Received: 15.06.2022

Revised: 30.06.2022

Accepted: 30.06.2022

Published: 30.06.2022



Use of recycled waste in the production of building materials

 Kapar Aryngazin¹,  Assem Abisheva^{2,*}

¹Department of Architecture and Design, Toraighyrov University, Pavlodar, Kazakhstan

²Department of Civil Engineering, L.N. Gumilyov Eurasian National University, Nur-Sultan, Kazakhstan

*Correspondence: abish_assem@mail.ru

Abstract. With the development of modern society, technological progress does not stand still. Mankind is constantly in search of new ideas and ways of implementation. This article of the authors is part of the modernization of the existing system of production of building materials. The authors propose to use secondary raw materials for the manufacture of a standard product, confirm them with laboratory tests and results. The indicators of the modified concrete mixture with the addition of ash-and-slag waste from the local industrial sector gave a density not inferior to the heavy concrete of 1.8 g/cm³. Positive effect is obtained by using hydraulic press, where at equal ratio of components due to pressing, all samples were transferred to a number of heavy concretes with a density of 1.8 to 2.5 g/cm³. Moreover, it was found that there are reserves of cement saving in the application of ash in the case of samples prepared by means of hydraulic press, as well as to correct the composition of concrete it is required to carry out a full-scale experiment with the joint action of vibration and pressing. Strength tests of samples show that there is an optimum quantity of ash and slag in the formulation, at that not only the standard requirements for the quality of construction products are met, but also exceeds some characteristics of products according to the requirements of standards.

Keywords: recycling, secondary raw materials, ash and slag waste, building materials, waste-free production, new materials.

1. Introduction

The development of modern society has formed a new kind of consumer, which has led to an increase in the rate of production in all sectors of the economy. This pattern can be seen in the intensity and acceleration of scientific and technological progress, which leads to the depletion of resources and minerals, as well as the negative impact on the environment. Despite this, the use of industrial waste is often criticized as well as supported. Non-waste technology is divided into two types. The first type is defined as the original material or semi-finished product for finished building materials or products. The second type is called secondary raw materials, which appeared as a consequence of the production of one product and can serve as initial raw materials for the second one. Common materials for recycling are: car tires, paper flour, construction debris, polymeric materials, which allows you to get crumb rubber, paper, crushed stone from recycled concrete, insulation materials and more [1].

The problematic topic of the use of industrial waste is the assessment of its market value. In this regard, the process of using secondary raw materials is divided into two stages. The first stage is the purchase of raw materials for processing, and the second stage is the production of secondary raw materials. An important role in all this is played by the quality of the primary recycled material, which should correspond to [2], where the norms of hard-to-recover losses and waste materials, which are reflected in the final cost of secondary raw materials. It is worth noting that recycling generates another volume, which is no longer suitable for use and requires more serious measures to eliminate. Thus, we can conclude that the lack of a clear systematic approach to assessing the value of secondary

raw materials and the industry as a whole cause a number of issues that require specific measures to eliminate them, as modern construction places high demands on the quality of the material while maintaining a low cost of production [3].

Among the CIS industrial giants, the Russian Federation alone has seen an increase in slag deposits of one million tons per year. These enterprises include thermal power plants, thermal power plants, coal enrichment, ferrous and nonferrous metallurgy. What not to say about the experience of foreign countries [4]. The way of using man-made materials as mineral raw materials is practiced in Poland, where metallurgical slags are exported to neighboring countries for the production of road pavement and construction materials [5]. In England ashes are used to partially replace cement and sand. In the USA ashes from thermal power plants are introduced into the concrete mixture in a certain ratio to cement to increase the density and sulfate value of concrete [6]. The experience of foreign countries in the use of ash is well described in [7], which concludes with a review of the current European standards [8-9], because the level of combustion products in the European Union countries is quite high (Figure 1).

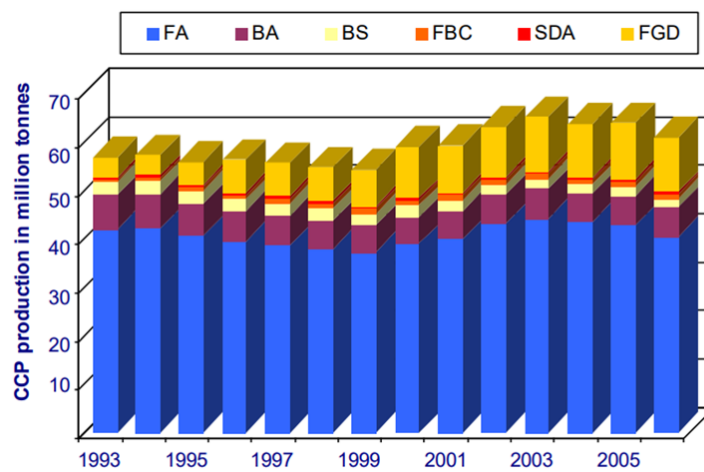


Figure 1 – Volumes of ash production in the EU [7]

The same analogy can be made based on the characteristics of the landfills of some rock dumps located in the Central Kazakhstan region. In essence, the ash contains 53 % of SiO₂, 24 % of Al₂O₃, 10 % of Fe₂O₃ and FeO, 2 % of CaO, 1 % of MgO, 4 % of oxides of alkali metals and 6 % of unburned fuel, which is often found in the composition of waste in rock dumps (Table 1).

Table 1 – Landfills of rock dumps of the Central Kazakhstan region

No.	Polygons	Area, ha	Hazard class	Amount of waste, tons/year	Total amount, tons	Waste composition, %
1	BGMK rock dumps, Kazakhmys Corporation, Sayak settlement	319	5	2397600	307305600	SiO ₂ – 74 CaCO ₃ – 21.5 MnCO ₃ – 3.8 Fe ₂ O ₃ – 0.3
2	BGMK rock dumps, Kazakhmys Corporation, Konyrat settlement	941	5	-	743898500	SiO ₂ – 54.4 Al ₂ O ₃ – 24.8 Fe ₂ O ₃ – 7.4 As – 0.002 Pb – 0.001
3	Vostochnaya Central Processing Plant rock dump, JSC IspatCarmet, Pridolinskiy settlement	70	5	99300	14432800	Zn – 0.004 Cu – 0.005 Gr – 0.0045 P – 0.06
4	Rock dump of ChOF, JSC IspatCarmet, Temirtau	159.9	5	844600	41356800	SiO ₂ – 60.2 Fe ₂ O ₃ – 5.73 Al ₂ O ₃ – 24.3

						Cu – 1.57
						MnO – 1.45
5	Rock dump Sh. Kazakhstanskaya, JSC IspatCarmet, Shakhtinsk	153	5	78600	35190000	As – 0.0002
						Pb – 0.003
						Zn – 0.01
						V – 0.015
						Mn – 0.15

Based on foreign experience, "Construction" is the only industry that is able to use the full potential of waste and by-products of other industries, which is the use of waste energy sector - ash and slag of Pavlodar CHPP-1, since the properties of ash is a fine material, which can be used as an additive to cement, aerated concrete, lime brick, and the chemical composition as mentioned above is identical to natural raw materials and can serve as a full and inexpensive alumina [10].

The involvement of any industrial sector allows to reduce the huge amount of space used for landfills and storage sites, which has a positive effect on the environment and the biosphere as a whole.

Thus, the Republic of Kazakhstan approved a program for the development of the construction industry and production of building materials for 2010-2014 [11], which states the favorable dynamics of development of the building materials industry, touched upon the issues of cost price and quality of materials. In this connection, a priority task was formed on the need for accelerated development of the basic sub-industries of cement, precast concrete, thermal insulation materials, glass, building ceramics, etc. with the maximum use of positive foreign experience and modern technology. The significance of the ongoing research is reflected in the second block: Energy saving in the production of powder, lumpy materials through the use of dispersed man-made products (ash, slag, slime, tailings, etc.), which substantiates the work of the authors of this article.

2. Methods

For the experiment, a formulation of mixtures for the industrial production of 3 types of building materials was developed: Paving slabs; Curbstone; Hollow stone.

The composition of the selected mixtures includes directly ash and slag waste (ASW) from thermal power plants and bauxite sludge from alumina production. Laboratory studies on the selection of the formulation are based on steelmaking slag from local steel mills and were carried out at the Independent Testing Center of Novosibirsk State Technical University.

The following materials were used as raw materials for the production of the studied samples of concrete:

- Sand [12];
- Portland cement PC-400-D20 [13];
- Fly ash from Pavlodar CHPP-1 (Table 2);
- Water [14].

Table 2 – Chemical composition of fly ash from Pavlodar CHPP-1

Components	Al ₂ O ₃	SiO ₂	Fe ₂ O ₃	CaO	MgO	K ₂ O	Na ₂ O	P ₂ O ₅	MnO	SO ₃
Contents, %	28.6	60.6	5.4	2	0.5	0.5	0.2	0.7	0.1	0.62

For the production of a basic sample of concrete Z0040, sand, Portland cement and water were used as materials. The base sample in terms of dry component included: 40% cement and 60% sand. The water-cement ratio was taken to be 0.35.

For the other series, each of which consisted of 6 samples, fly ash was introduced by replacing sand and Portland cement in 10 % increments, with 5 % of the sand and 5 % of the Portland cement being replaced. Dry components were mixed together, then water was added. The composition of the resulting concrete mixtures is shown in the graph (Figure 2).

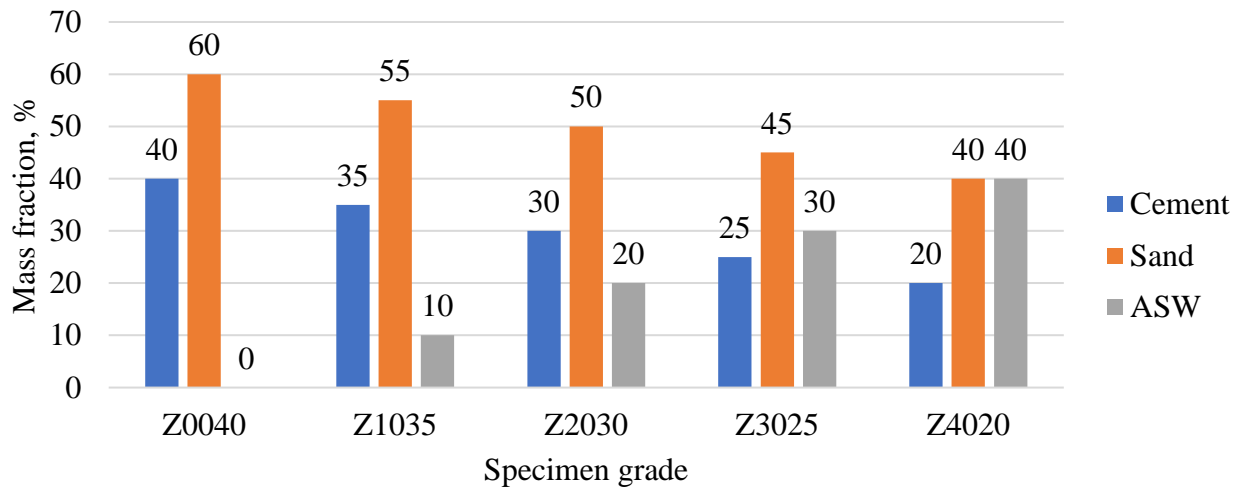


Figure 2 – Compositions of concrete mixtures using ASW

The vibropress designed for pressure of 100 kg/cm² (10 MPa) and vibration frequency of 50 s⁻¹ with an amplitude of 0.35-0.5 mm was used for the experiment.

The first stage of the experiment uses a vibration table (VT) with a vibration frequency of 3000 rpm at an amplitude of 0.4 mm. For the experiments, cube shapes 100x100x100 mm with the bottom were used (Figure 3). Determination of the density of concrete samples was carried out in accordance with [15].



Figure 3 – Samples of cubes after the vibrating table

At the second stage of the experiment a hydraulic press (HP) PGM -100MG4 was used, but in this case, cube shapes 100x100x100 mm without the bottom were used, the composition of the concrete mixture was identical to the first (Figure 4).



Figure 4 – Samples of cubes after the hydraulic press

Next, a P-10 press was used to determine the strength characteristics of concrete cube samples at 28 days of age (Figure 5).



Figure 5 – Hydraulic press testing process

3. Results and Discussion

The graph below shows that the density of concrete decreases as the percentage of the mass component of ash in the concrete mixture increases. Samples Z0040 and Z1035 have a density above 1.8 g/cm^3 , so they belong to the class of heavy concrete. Samples of grades Z2030, Z3025, Z4020 can be attributed to the class of lightweight concrete (Figure 6).

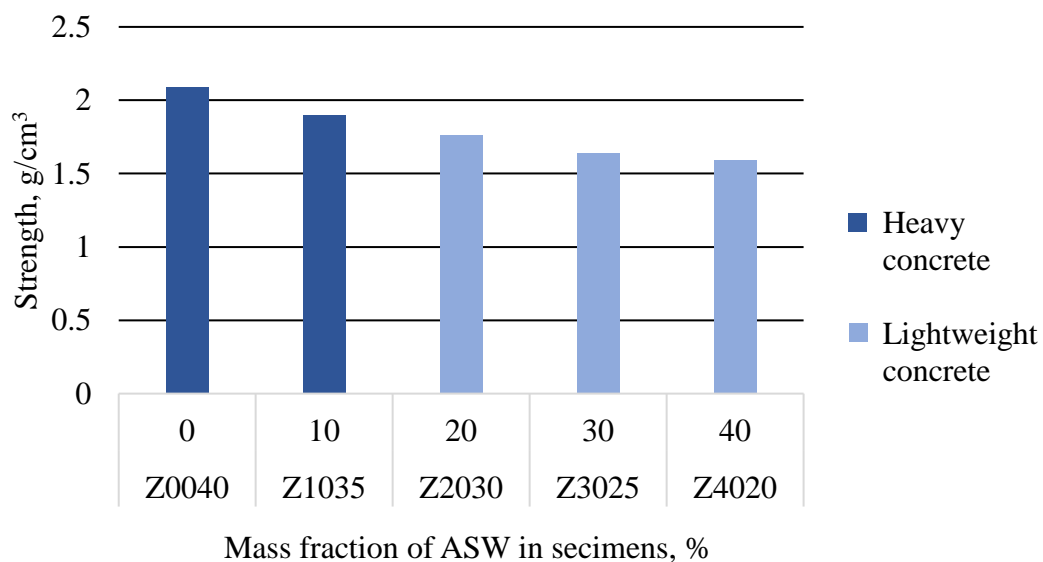


Figure 6 – Density of concrete samples obtained after using the vibrating table

After using the hydraulic press PGM, noticeably, the density of concrete samples became higher than at the first stage of the experiment, on average 1.2 times. Now all samples belong to the heavy class of concrete (Figure 7).

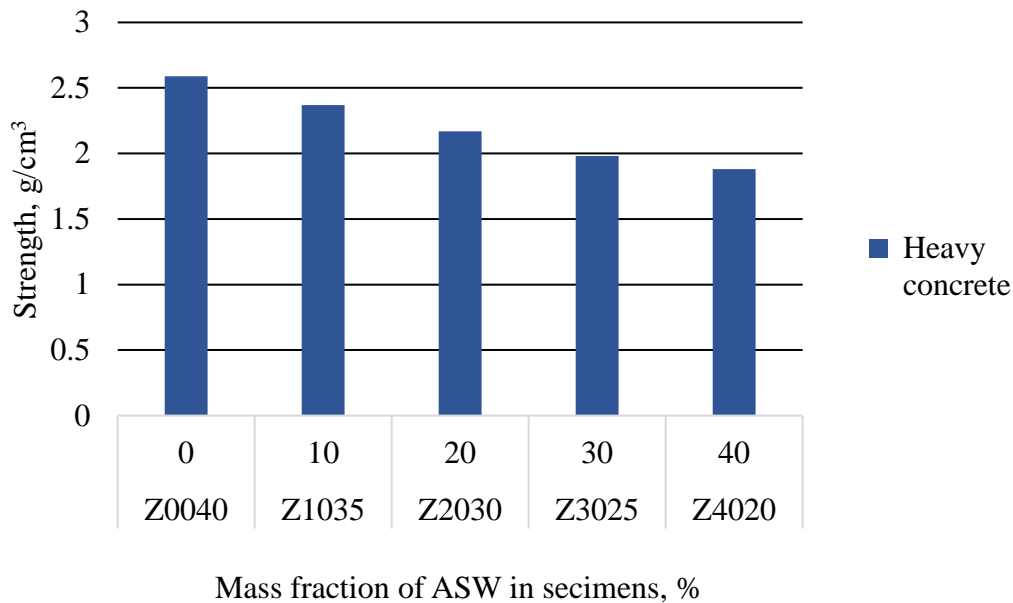


Figure 7 – Density of concrete samples prepared on a hydraulic press

The use of ash is based on a number of its physical and chemical properties, namely on its pozzolanic activity. This refers to the ability of ash to interact with calcium hydroxide and alkalis in the pore fluid of concrete [16]. There is an opinion that ash is an ideal binder for reinforced concrete products and factory-type structures [17].

According to the results of experiments, it can be argued about the sufficient strength gain of compositions for the manufacture of products with the addition of ash-and-slag mixtures to the concrete mixture.

4. Conclusions

On the basis of tests of samples using ash and slag from Pavlodar CHPP-1 it was found that:

- There are reserves of cement savings in the application of ash in the case of preparing samples using a hydraulic press.
- To adjust the composition of concrete it is required to conduct a full-scale experiment with the joint action of vibration and pressing.

Strength tests of samples show that there is an optimum quantity of ash and slag in the formulation, at those not only standard requirements to the quality of building products are met, but also exceeds some characteristics of products according to the requirements of standards.

Acknowledgments

This study was funded by the Ministry of Digital Development, Innovations and Aerospace Industry of the Republic of Kazakhstan and World Bank (Grant No. APP-SSG-17/0290F).

References

1. Features of the production of cement asphalt concrete using fuel ash / K. Aryngazin, M. Zhulasheva, A. Abisheva, A. Takirova, D. Aligozhina // *Technobius*. — 2022. — Vol. 2, No. 1. — P. 0012. <https://doi.org/10.54355/tbus/2.1.2022.0012>
2. RDS 82-202-96 Guide to the Development and Application of Standards for Hard-To-Avoid Losses and Material Wastes in Building Construction [Electronic resource] / Tulaorgstroy // *Meganorm*. — [2021]. — Mode of access: <https://meganorm.ru/Index2/1/4294854/4294854574.htm> (accessed date: 01.06.2022).
3. Increasing coal combustion product utilization in Russia as a crossindustry goal / P. Snikkars, I. Zolotova, N. Osokin // *Energy Policy*. — 2020. — No. 7. — P. 34-45. https://doi.org/10.46920/2409-5516_2020_7149_34

4. Analyzing the Technology of Using Ash and Slag Waste from Thermal Power Plants in the Production of Building Ceramics / A.G. Malchik, S.V. Litovkin, P.V. Rodionov, V.V. Kozik, M.A. Gaydamak // IOP Conference Series: Materials Science and Engineering. — 2016. — Vol. 127. — P. 012024. <https://doi.org/10.1088/1757-899X/127/1/012024>
5. Construction materials from ash and slag waste [Electronic resource] / ECTC // Engineering Chemical Technology Center. — [2022]. — Mode of access: <https://ect-center.com/blog/stroymaty-iz-othodov> (accessed date: 01.06.2022).
6. Ispolzovanie othodov promyshlennogo proizvodstva pri izgotovlenii stroitelnykh izdelij i materialov / I.V. Zabornikova, Ye.D. Podgornaya // Scientific Collection «Interconf»: Vol. 2(35): Experimental and theoretical research in modern science. — Kishiniev, Moldova: 2020. — P. 509-514.
7. Calcareous Ash in Europe - a reflection on technical and legal issues / H.-J. Feuerborn // 2nd Hellenic Conference on Utilisation of Industrial By-Products in Construction, EVIPAR. — Aiani Kozani, Greece: 2009. — P. 3.
8. EN 450-1:2012 Fly ash for concrete - Part 1: Definition, specifications and conformity criteria [Electronic resource] / CEN // iTeh Standards Store. — [2012]. — Mode of access: <https://standards.iteh.ai/catalog/standards/cen/cc9c0d2c-6d67-4290-82ea-e5e99eb8abf0/en-450-1-2012> (accessed date: 01.06.2022).
9. EN 450-2:2005 Fly ash for concrete - Part 2: Conformity evaluation [Electronic resource] / CEN // iTeh Standards Store. — [2005]. — Mode of access: <https://standards.iteh.ai/catalog/standards/cen/51739f75-d717-4dd9-9f2c-779819cb4a6e/en-450-2-2005> (accessed date: 02.06.2022).
10. Promyshlennaya ekologiya / O.A. Fedyeva. — Omsk, Russia: OmGTU, 2007. — 145 p.
11. Ob utverzhdenii Programmy po razvitiyu stroitelnoj industrii i proizvodstva stroitelnykh materialov v Respublike Kazahstan na 2010 - 2014 gody [Electronic resource] / adilet.zan.kz // Informacionno-pravovaya sistema normativnykh pravovykh aktov Respubliki Kazahstan. — [2010]. — Mode of access: <https://adilet.zan.kz/rus/docs/P1000001004> (accessed date: 01.06.2022).
12. GOST 8736-2014 Sand for construction works. Specifications [Electronic resource] / Standardinform // Meganorm. — [2021]. — Mode of access: <https://meganorm.ru/Index2/1/4293767/4293767502.htm> (accessed date: 02.06.2022).
13. GOST 10178-85 Portland cement and portland blastfurnace slag cement. Specifications [Electronic resource] / Gosstroy // Meganorm. — [2021]. — Mode of access: <https://meganorm.ru/Index2/1/4294853/4294853156.htm> (accessed date: 02.06.2022).
14. GOST 23732-2011 Water for concrete and mortars. Specifications [Electronic resource] / Standardinform // Paragraph. — [2011]. — Mode of access: https://online.zakon.kz/Document/?doc_id=31335909 (accessed date: 02.06.2022).
15. GOST 12730.1-78 Concretes. Methods of determination of density [Electronic resource] / Standardinform // Paragraph. — [2018]. — Mode of access: https://online.zakon.kz/Document/?doc_id=30039457 (accessed date: 02.06.2022).
16. Biomass fly ash in concrete: Mixture proportioning and mechanical properties / S. Wang, A. Miller, E. Llamazos, F. Fonseca, L. Baxter // Fuel. — 2008. — Vol. 87, No. 3. — P. 365–371. <https://doi.org/10.1016/j.fuel.2007.05.026>
17. Worldwide production of coal ash and utilization in concrete and other products / O.E. Manz // Fuel. — 1997. — Vol. 76, No. 8. — P. 691-696. [https://doi.org/10.1016/S0016-2361\(96\)00215-3](https://doi.org/10.1016/S0016-2361(96)00215-3)

Information about authors:

Kapar Aryngazin – Candidate of Technical Sciences, Professor, Department of Architecture and Design, Toraighyrov University, Pavlodar, Kazakhstan, kapar2021@gmail.com

Assem Abisheva – PhD Student, Department of Civil Engineering, L.N. Gumilyov Eurasian National University, Nur-Sultan, Kazakhstan, abish_assem@mail.ru

Author Contributions:

Kapar Aryngazin – concept, methodology, resources, interpretation, editing, funding acquisition.

Assem Abisheva – data collection, testing, modeling, analysis, drafting, visualization.

Received: 20.06.2022

Revised: 30.06.2022

Accepted: 30.06.2022

Published: 30.06.2022